ITERATIVE SC-FDMA FREQUENCY DOMAIN EQUALIZATION & PHASE NOISE MITIGATION

BY

MOHAMED ANBAR MOHAMED OMAR

A Thesis Presented to the
DEANSHIP OF GRADUATE STUDIES

KING FAHD UNIVERSITY OF PETROLEUM & MINERALS
DHAHRAN, SAUDI ARABIA

In Partial Fulfillment of the
Requirements for the Degree of

MASTER OF SCIENCE

In

ELECTRICAL ENGINEERING

May 2018

KING FAHD UNIVERSITY OF PETROLEUM & MINERALS

DHAHRAN- 31261, SAUDI ARABIA

DEANSHIP OF GRADUATE STUDIES

This thesis, written by **MOHAMED ANBAR MOHAMED OMAR** under the direction of his thesis advisor and approved by his thesis committee, has been presented and accepted by the Dean of Graduate Studies, in partial fulfillment of the requirements for the degree of **MASTER OF SCIENCE IN ELECTRICAL ENGINEERING.**

Thesis Committee

Dr. Azzedine Zerguine (Advisor)

Dr. Naveed Iqbal (Member)

Dr. Ali Nasir (Member)

Dr. Ali A. Al-Shaikhi

Department Chairman

Dr. Salam A. Zummo
Dean of Graduate Studies

21/5/13

Date

To those who pushed me all the way from the start to the end of the road, To the soul of my father, my mother, my wife, my son, my brothers and my sisters

ACKNOWLEDGMENTS

To Allah belongs all praise -lord of the heavens and Lord of the earth, Lord of the worlds, for the good health and well-being that were necessary to complete this work.

I would like to express my sincere gratitude to my advisor Dr. Azzedine Zerguine for the continuous support during my master study and related research. He was always available to answer my questions and assist me in analyzing the data. Without his excellent guidance, patience, caring, and motivation, this work would not have been finished.

I am also deeply grateful to my thesis committee members; Dr. Naveed Iqbal and Dr. Ali Nasir for their constructive comments, suggestions and continuous support. Dr. Iqbal have been very cooperative in clarifying some important issues of this work.

I would also like to think my brothers, sisters, and my beloved wife. They were always supporting me and encouraging me with their best wishes.

Thanks for all the Egyptian community in KFUPM for their support.

Finally, I would like to express my thanks to the Electrical Engineering Department and King Fahd University of Petroleum and Minerals for their support to accomplish this piece of work.

TABLE OF CONTENTS

LIST OF TABLES

LIST OF FIGURES

LIST OF ACRONYMS

ISI	Inter Symbol Interference
SC	Single Carrier
MC	Multi Carrier
LE	Linear Equalization
DFE	Decision Feedback Equalizer
MLSE	Maximum Likelihood Sequence Estimation
OFDM	Orthogonal Frequency Division Multiplexing
SC-FDE	Single Carrier Frequency Domain Equalization
SC-FDMA	Single Carrier Frequency Division Multiple Access
PHN	Phase Noise
QAM	Quadrature Amplitude Modulation
PAM	Pulse Amplitude Modulation
PAPR	Peak to Average Power Ratio
MMSE	Minimum Mean Square Error
ZF	Zero Forcing
LO	Local Oscillator

LIST OF ABBREVIATIONS

Δf	Sub-carrier spacing
T	Symbol period
$\mathrm{H}(\omega)$	Channel's frequency response
$f(\omega)_{zf}$	Zero forcing filter frequency response
$f(\omega)_{mmse}$	Minimum mean square error filter frequency response
N_o	Noise power spectral density
σ_n^2	Noise variance
σ_s^2	Signal variance
f_c	carrier frequency
$L(f_m)$	PHN SSB power spectrum density
f_m	Offset frequency from the carrier frequency
p_{signal}	Signal power
p_{noise}	Noise power
N_u	Number of system users
M	Number of system subcarriers
N	Number of system subcarriers assigned to only one user

L_{ch}	Channel impulse response length
$\boldsymbol{T_k}$	Is an $M \times N$ sub-carrier mapping matrix
$\boldsymbol{s_k}$	Is the $(N \times 1)$ symbol vector of the K^{th}user
$\boldsymbol{F_N}$	The FFT matrix with dimensions $(N \times N)$
$\boldsymbol{F_M^H}$	The IFFT matrix with dimensions $(M \times M)$
$\boldsymbol{g_k}$	Time domain transmitted vector to the K^{th}user
h_k	The $(L_{ch} \times 1)$ impulse response of the channel
r^t	t^{th} SC-FDMA time domain received signals corresponding to all N_u users
$\boldsymbol{H_l^{th}}$	The $(M \times M)$ channel circular convolution matrix in time domain
$\boldsymbol{n^{th}}$	The $(M \times 1)$ AWGN vector
R^t	t^{th} SC-FDMA frequency domain received signals corresponding to all N_u Users
$\boldsymbol{\widehat{H}_l}$	The $(M \times M)$ channel diagonal matrix in frequency domain
$\boldsymbol{T_k^H}$	Is an $M \times N$ sub-carrier demapping matrix
$\boldsymbol{\overline{\widehat{H}}_k}$	Is A $(N \times N)$ sub-matrix of $(M \times M)$ $\widehat{H}_k$ matrix.
N_L	Number of iterations
F_L	Feedforward filter coefficients

B_L	Feedback filter coefficients
u_i^L	The i^{th}output of the equalizer in time domain at the L^{th} iteration
$\widehat{\boldsymbol{S}}$	The estimated output of the equalizer in frequency domain.
β	Beta coefficient
$\sigma^2_{\hat{s}_{L-1}}$	Estimated signal variance at the L^{th} iteration
$r_{s,\hat{s}_{L-1}}$	Correlation estimation at the L^{th} iteration
$\boldsymbol{\delta_r^t}$	Transmitter diagonal PHN matrix
$\boldsymbol{\delta_l^t}$	Receiver diagonal PHN matrix
$\emptyset_b^{t,r}$	RX PHN sample affecting the t^{th} SC-FDMA TD Symbol at b^{th} sample
$\emptyset_b^{t,l}$	TX PHN sample affecting the t^{th} SC-FDMA TD symbol at b^{th} sample
$\boldsymbol{\gamma_b^{t,r}}$ & $\boldsymbol{\gamma_b^{t,l}}$	i.i.d Gaussian random variables
$R(n)$	Reliability metric
$\lfloor \hat{S} \rceil$	Rounding to the nearest constellation point
$\lfloor \hat{S} \rceil_{NN}$	Rounding to the next nearest constellation point
$(.)_{R,i}$	Denote the in-phase components
$(.)_{I,i}$	Denote the quadrature components

$E[s_{R,i}e^{*}{}_{R,i}]$ The error and transmitted symbol expectation

$p(e^{j*}{}_{R,i})$ Quadrature component error probability

$p(e^{j*}{}_{R,i})$ Quadrature component symbol a priori probability

$p(e^{j*}{}_{R,i}/s^{k}{}_{R,i})$ Quadrature component of conditional error probability

$\gamma_{s\ PAM}$ SNR per symbol for PAM constellation

$\gamma_{s\ QAM}$ SNR per symbol for QAM constellation

ABSTRACT

Full Name : Mohamed Anbar Mohamed Omar

Thesis Title : Iterative SC-FDMA Frequency Domain Equalization & Phase Noise Mitigation

Major Field : Electrical Engineering

Date of Degree : May 2018

The presence of natural and man-made objects made the transmitted signals simultaneously travel over multi-paths to the receiver. Each signal arriving along each path suffering from different attenuations and propagation delays. The multipath channel will generate intersymbol interference (ISI) between the transmitted symbols. When the symbol period becomes shorter than the period of dispersion, that makes it very hard to reproduce symbols at the receiver. Increasing the transmission rate is always one of the basic objects for the development of the new wireless communication techniques but this will increase ISI at the receiver side. Accordingly, how to restore symbols damaged by ISI is an essential point in wireless systems. To alleviate the harmful effects of ISI, equalization is generally used.

One of the principal radio frequency (RF) impairments that generate shifts of the transmitter and receiver oscillators signals, and emerging from errors in the fabrication process of the local oscillator (LO), is a random process called phase noise (PHN). In SC-FDMA PHN impact every symbol by very little rotation, in addition, to stretch the energy of all of the subcarriers over each other and consequently produces a harmful effect on the system's performance. PHN influences and considerations must be accurately analyzed and examined when creating a standard wireless communication system because a reliable

forecasting of the acceptable PHN level allow the wireless communication schemes and RF designers to relax specifications.

A Discrete Fourier Transform (DFT) precoded OFDM scheme called the Single-Carrier-FDMA (SC-FDMA) is an excellent design that has been adopted for uplink transmission in the Long-Term Evolution (LTE) standard. The presence of LO impairments (PHN) and bad environment (deep fading), if not taken into account, have deleterious effects on the performance of the SC-FDMA system. In this thesis, we propose a new approach to mitigate both of the PHN and the deep fading effects in the SC-FDMA system iteratively. This is achieved by exploiting the nature of the PHN in both time and frequency domains in addition to the iterative nature of the frequency domain equalization algorithm. Also, we will propose a novel two approaches to alleviate the error propagation in the decision feedback. Our simulation results prove our findings in a vehicular A channel model.

ملخص الرسالة

الاسم الكامل : محمد عنبر محمد عمر

عنوان الرسالة: التسوية الترددية ومكافحة التشوش الطورى للنظام احادى القناة بطريقة التكرار .

التخصص:هندسة كهربائية

تاريخ الدرجة العلمية : مايوم 2018

في أنظمة الاتصالات الممتازة ، تكون البيانات المستلمة متطابقة مع البيانات المرسلة. ومع ذلك ، ليس هذا هو الحال بالنسبة لأنظمة الاتصالات الحقيقية حيث في أنظمة الاتصالات اللاسلكية وجود الأشياء الطبيعية والتي من صنع الإنسان يجعل الإشارات المرسلة تنتقل في الوقت نفسه عبر مسارات متعددة إلى المستقبل.كل أشارة تصل على مسار معين تعانى من توهين وتاخير مختلفين . وتتمثل القضية الناتجة في تشتت الإشارة المرسلة عبر القناة متعددة المسارات.سوف تقوم القناة متعددة المسارات بتوليد (ISI) تداخل بين الرموز المرسلة عندما تكون الفترة الزمنية للرمز اصغر من الفترة الزمنية لتشتت القناة مما يجعل من الصعب جدا اعادة توليد الرموز مرة اخرى عند المستقبل. إن زيادة معدل الإرسال والموثوقية هي دائمًا أحد الأشياء الأساسية لتطوير تقنيات الاتصال اللاسلكي. علاوة على ذلك ، للحصول على معدل إرسال عالي ، تكون معدلات الرموز العالية ضرورية وهذا يقلل من مدة الرموز بالمقارنة مع تشتت القناة مما يؤدى الى مزيد من التداخل (ISI) عند المستقبل . وفقا لذلك، فكيفية استعادة الرموز التي تضررت من (ISI) هي النقطة الأساسية في الأنظمة اللاسلكية. للتخفيف من الآثار الضارة لل(ISI) يتم استخدام التسوية بشكل عام .وقد أعطيت كمية ضخمة من البحوث لتحسين تقنيات التسوية العملية.

إن إحدى عوائق التردد الراديوي الرئيسية التي تولد تغيرات في إشارات المستقبِلات وأجهزة إرسال المرسلات ، والناشئة من أخطاء في عملية تصنيع المزبزب المحلى ، العملية العشوائية التى تسمى ضوضاء الطور .تؤثر الضوضاء الطورية فى انظمة الاتصالات احادية القناة (SC-FDMA) بازحة زاوية كل رمز على حدة بالاضافة الى تمتد طاقة جميع الموجات الحاملة الفرعية فوق بعضها البعض وبالتالي تنتج تأثيرًا ضارًا على أداء النظام. يجب تحليل تأثيرات الضوضاء الطورية بدقة وفحصها عند إنشاء نظام اتصالات لاسلكي قياسي لأن التنبؤ الموثوق به

لمستويات الضوضاء الطورية المقبولة يسمح لمخططات الاتصالات اللاسلكية ومصممي الترددات اللاسلكية بتحقيق المواصفات اللازمة .

في هذه الأطروحة ، نقترح أولاً الجمع بين التسوية الترددية والتعويض الطورى للنظام احادى القناة بصفة تكرارية اعتمادا على الانظمة التكرارية للتسوية الموجودة فى الادبيات .ثم بعد ذلك نقوم بعمل تحسين لطريقة التسوية عن طريق التغلب على معضلة الاخطاء المنتشرة اعتمادا على موثوقية الرموز المكتشفة العكسية . و بما أن الفكرة الأساسية لتحسين أداء التسوية التكرارية الترددية يعتمد على موثوقية الرموز العكسية التى تكون مختفية عند المستقبل فانه سوف يتم تقديم إجراءات حسابية للموثوقية.

CHAPTER 1

INTRODUCTION

In this chapter a brief overview of Single-carrier (SC) and Multi-carrier (MC) multiple access techniques was investigated. Also, present the effect of fading channel and Phase Noise (PHN) in the wireless systems and how to tackle these problems.

1.1. Signal and Multi-carrier Access Communication Schemes

One of the proposed solutions that have gained much attention in the last few years to mitigate the frequency-selective fading dilemma in wireless systems is the utilization of MC technology. MC technique divides the entire spectrum into smaller channels; high rate stream into parallel low rate sub-streams. No complicated equalization and high spectral efficiency were the motivations for utilizing this technology.

1.1.1. OFDM System

Orthogonal frequency division multiplexing (OFDM) is essentially an information representation technique, with the principle aim of facilitating simple baseband transceiver structure. OFDM is simply the very common defined scheme of multicarrier techniques, which uses orthogonal subcarriers to convey information.

In the frequency domain (FD), the carrier spacing is accurately selected where the coherence bandwidth of the channel BW_{ch} becomes relatively more than the spectrum assigned to every sub-carrier Δf. Therefore, each sub-carrier will be affected by a flat fading. This facilitates the equalization process by trivial one-tap filter, unlike wideband communication systems which suffer from selective fading and require complex equalization. In addition, all sub-carriers are orthogonal to each other, where the magnitude

of each sub-carrier has zero value at the center frequency of each of the other sub-carriers as shown in Fig.1.1 and consequently this results in no interference between adjacent sub-carriers.

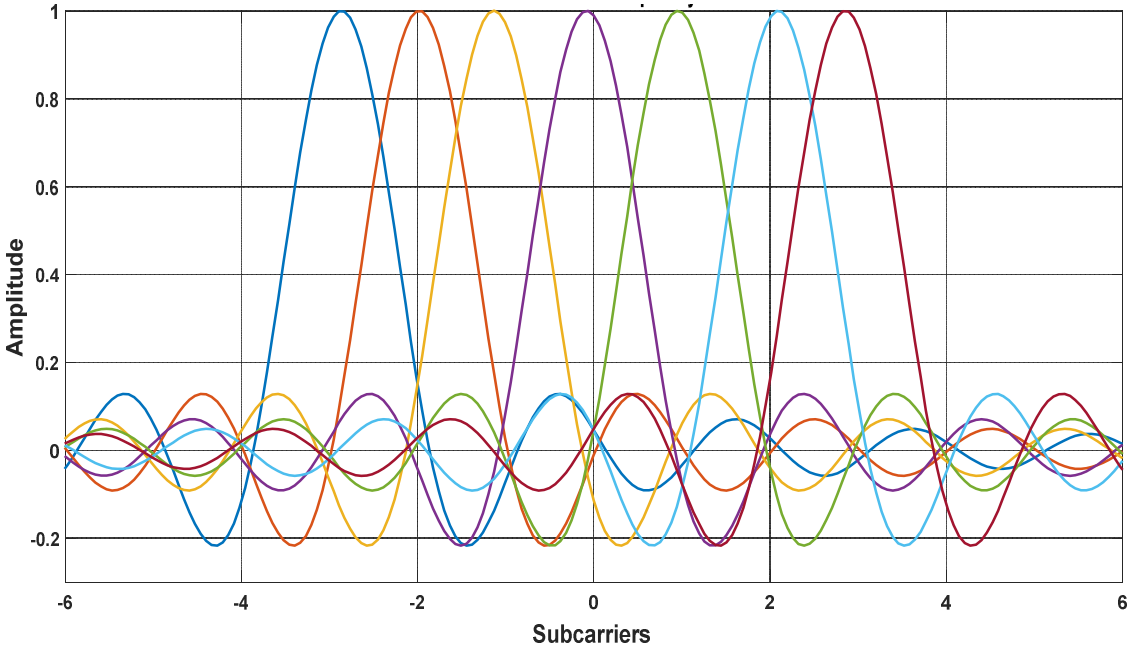

Figure 1.1: OFDM system Orthogonal Subcarriers .

By dividing the high rate stream into parallel lower rates, as shown in Fig.1.2, OFDM overcomes the problem of inter-symbol-interference (ISI) made by multipath fading in the wireless wideband communication channels, where the transmitted symbol period T become more than the channel delay spread. In OFDM, the symbol period T of each particular sub-carrier is related to the sub-carrier spacing Δf by

$$\Delta f = \frac{1}{\mathrm{T}}. \tag{1.1}$$

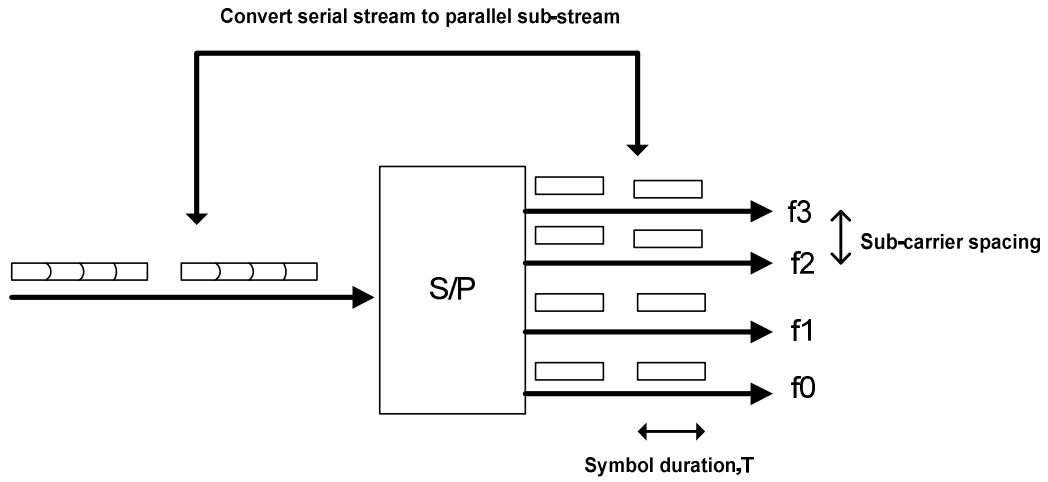

Figure 1.2: OFDM sub carriers mapping.

In an OFDM transmitter, as shown in Fig.1.3, the high data rate bit stream crosses through the chosen modulation scheme (e.g., a QAM modulator). The modulated symbols are serial to parallel transformed and treated by the Inverse Fast Fourier Transform (IFFT). The modulator output signal can be seen as complex data symbols in the FD, then we use the IFFT to obtain the OFDM signal in the TD. IFFT multiplex data into parallel sub-carriers. There is a one-to-one mapping between symbols and sub-carriers. Finally, the guard period is added and a P/S adaptor is utilized, whose output is the baseband OFDM signal. A guard period is utilized between OFDM symbols to prevent the inter-block-interference (IBI) and convert the linear convolution between the transmitted signal and channel to circular convolution for equalization purposes at the receiver. In LTE, this guard period is named as a Cyclic Prefix, with a period longer than the impulse response of the channel and identical to the last portion of the OFDM block.

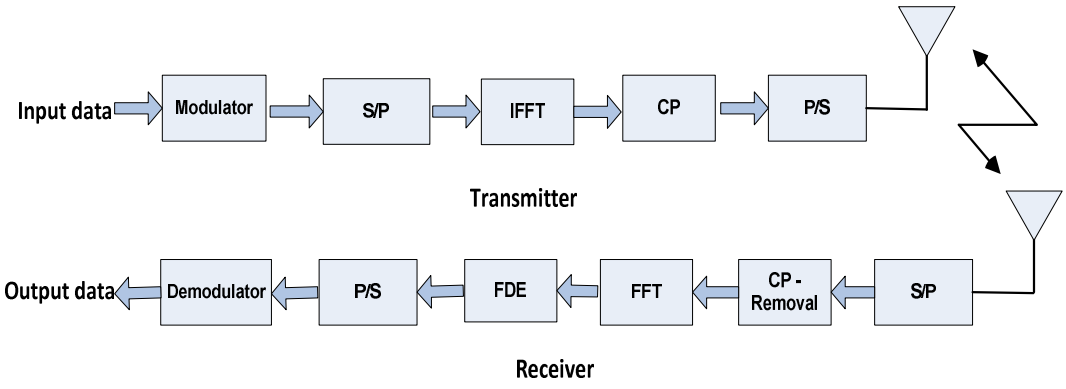

Figure 1.3: OFDM system architecture.

The receiver performs exactly what was done at the transmitter but in opposite direction. The CP is removed first, then the FFT transforms the OFDM symbols into FD accompanied by equalizer and demodulator as shown in Fig. 3. More details on the OFDM system architecture can be found in [1]–[6].

The significant benefits of the OFDM system can be summarized as follows:

- Great spectral efficiency where the handled orthogonal sub-carriers are overlapped in the frequency domain.
- Utilization of the DSP algorithms like the FFT, which improve the overall system's efficiency.
- Various modulation techniques can be done on particular subcarriers, which are adjusted to the SNR of the individual subcarrier.

Due to these benefits, OFDM system has been approved as a modulation scheme in various communication systems such as IEEE 802.11 (WLANs) and DVB-T (Digital Video Broadcasting-Terrestrial) [6].

Also, an OFDM system suffers from the following drawbacks [7]:

- Since OFDM is a MC transmission technique, it is extremely sensitive to synchronization mismatches like frequency offsets (FO) and phase noise (PHN), and eventually destroy the orthogonality between adjacent sub-carriers and generate intercarrier interference (ICI).
- Sensitivity to the resolution and dynamic range of (A/D) and (D/A) converters, due to the suffering from high peak-to-average power ratio (PAPR).
- High PAPR, where the transmitted OFDM signal, resulted from the summation of many subcarriers, each with its own frequency, generates a signal with a wide dynamic range, with an almost high PAPR. This leads to degrading the efficiency of the used power amplifier (PA).

1.1.2. OFDMA System

OFDMA is a multiple access (MA) scheme of OFDM [8], [9] to serve many users at the same time with the same features of OFDM. Each user is served with a small number of sub-carriers to communicate through a specific time. Generally, subcarriers are specified to each user in adjacent groups, for uniformity and to decrease the cost of showing which subcarriers have been assigned to each user. One of the vital restrictions with an OFDMA method is to synchronize the uplink (UL) transmission so that, each user circumvents in sending its frame to avoid interfering with the other users. The OFDMA style for portable communications was initially proposed in[10] based on MC-FDMA, where every user was served with a specified set of randomly chosen subcarriers.

While OFDMA is deployed employed in the LTE down-link (DL) scenario, and own significant benefits as opposed to those of the MA techniques of the early mobile communication systems, it doesn't face the difficulties of the LTE uplink (UL), where the transmitter, in this case, is the mobile station (MS) and the transmitted power should be under some specified threshold. This condition arises from the fact that an OFDM signal has a high PAPR and this lead to a high-power consumption and a high signal distortion.

1.1.3. SC-FDE System

Today, Single Carrier Frequency Domain Equalization (SC-FDE) system can be seen as an alternative option to OFDM to combat the selectivity of the channel. It has a comparable performance and complexity to OFDM while circumventing some restrictions, such as great PARP. Single carrier systems have significantly moderate PAPRs, which particularly are the important issue for the uplink transmission. In wireless communication systems, the uplink transmissions are usually restricted by the power of the terminal units (MS) and interferences. Therefore, the mobile terminals necessitate transmitting data at the lowest potential power over kilometers of distance[11].

Additionally, traditional time domain equalization for broadband multipath channels is ineffective because the channel impulse response in TD is very tall and this increases the equalization complexity. FD equalization is more powerful for such channels, where the DFT components do not increase linearly with the channel length.

A system structure can be seen in Fig1.4 at the transmitter side, a CP attached to the partitioned data sequences with length N as in OFDM system to combat Inter Block Interference (IBI) and allow the use of circular convolution with the channel instead of linear.

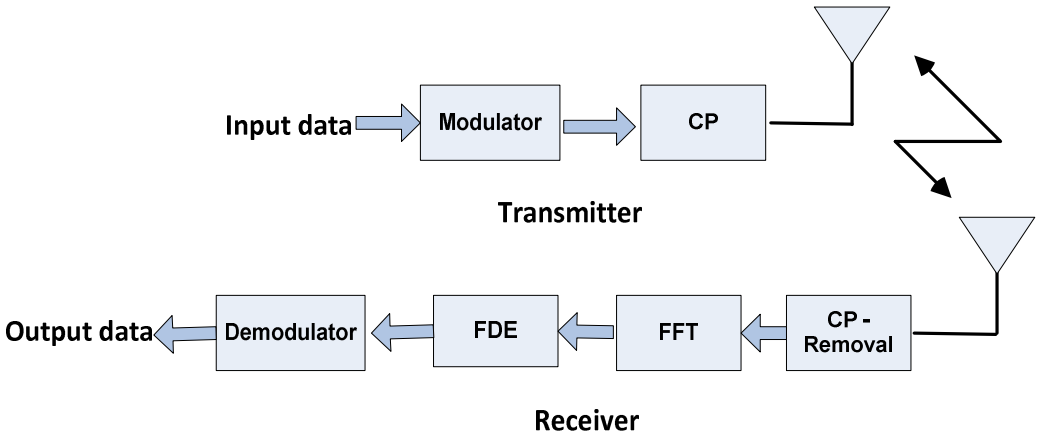

Figure 1.4: SC-FDE system architecture.

The main data of SC-FDE is in time domain format, unlike OFDM which is in frequency domain. After the transmission, the data circularly convolved with the wireless channel. Then, the SC-FDE receiver converts the received data to frequency domain by FFT, after discarding the CP component. Then, a FD equalizer is used in the hope to invert the channel's response. Equalization and channel filtering must have the equivalent type of convolution, either linear or circular convolution, since we are using FFT to obtain FD transformation we should have circular convolution in TD should be used, which is done using CP. Then the data is converted again to the TD for decoding. This is still SC system with equalization in FD, where single carrier transmission is used. Most of the well-known TD-E techniques, like MMSE and DFE can be employed to the FD-E. The features of the FD implementation of these equalizers well presented in [12]–[17].

By distinguishing between the two schemes in Figures 1.3 and 1.4, it is exciting to observe that, the two constructions surely exhibit a number of similarities. Overall, they both use the equivalent functional transmission with a CP and utilize the FFT to raise the

efficiency. The principal contrast between them is in the employment of the FFT and IFFT operations.

In an OFDM system, an IFFT functional block is located at the transmitter side in order to multiplex stream of data into parallel subcarriers and an FFT functional block is located at the receiver side for FD equalization, while in the SC-FDE, both IFFT and FFT functional blocks are located at the receiver side for FD equalization. Therefore, one can anticipate that the two methods will have in like manner coded representations and computational complexity.

Nevertheless, there are notable distinctions that make the two approaches work differently. In OFDM, the detection of data is performed per-subcarrier basis in the FD, while the detection in SC-FDE is performed in TD after IFFT operation. Due to this diversity, OFDM becomes higher critical to nulls in the spectrum and need coding of the channel to overcome this weakness. Also, the place of IFFT has amazing exciting results to distinguish between them. In particular, the primary data for SC-FDE is in the TD, while it is in FD for OFDM. This allows OFDM to be more resilient than SC-FDE in data positioning. where the data with more quality placed adaptively in a great excellent section of the available subcarriers, while the data with limited quality placed in the bad one. In this way, we can gain frequency diversity.

***In brief, single carrier FDE has attractive benefits over OFDM as follows*:**

- Moderate PAPR, since there isn't IFFT functional block at the transmitter and utilizing SC modulation.
- Durability to spectral null.

- Moderate sensitivity to CFO.
- Both CP and data are in the TD and we can use a training sequence in place of CP to perform channel state estimation (CSE) and timing synchronization with a slight reduction in efficiency.
- Reducing the consumed power at the transmitter side due to the moderate computational complexity.

Notwithstanding, the variations discussed above, the two schemes are very close to each other. Truly, a mixture scheme for the cellular system has recommended, employing OFDM for downlink (DL) and SC-FDE for the uplink (UL). As a result, most of the signal processing will be done at the BS leaving less to do with the MS. The integral characteristics of the two schemes execute an excellent combination for this scenario[18].

1.1.4. SC-FDMA System

To accommodate multiple users, SC-FDE was modified to Single-Carrier FDMA. SC-FDMA utilizes SC modulation and FD-E, based on the identical concept as SC-FDE. SC-FDMA produces comparable performance and approximately similar complexity as those of OFDMA [7]. Consequently, SC-FDMA is introduced as the DFT-spread OFDM. Also, it catches a great interest as an alternative choice to OFDMA, particularly in the UL of the wireless cellular standards, where its inherent single carrier structure gives a signal with low envelope fluctuations (lower PAPR) less energy consumption of the PA and greatly serves the MS in terms of power efficiency and manufacturing cost. This point makes the employment of SC-FDMA scheme in the LTE system UL very promising.

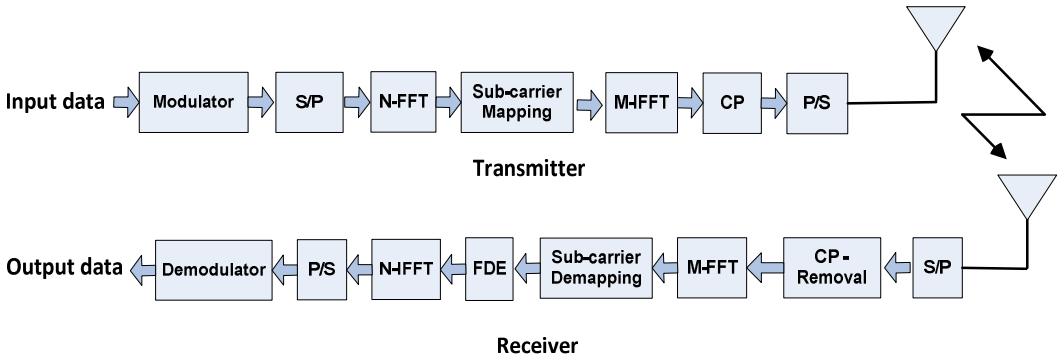

Figure 1.5: SC-FDMA system diagram.

AS we can see from Fig.1.5, the SC-FDMA has greatly common features with the OFDMA such as orthogonal sub-carriers FD multiplexing\demultiplexing and FD-E, except for the additional FFT and IFFT blocks in the transmitter and receiver, respectively, and SC transmission. The TD symbols in SC-FDMA are transformed to FD by N-FFT, then the subcarrier mapper maps each output of the FFT to one of the M subcarriers before passing through the OFDMA. There are two traditional mapping styles in SC-FDMA, localized mapping style and distributed style. When the user's data utilize a set of separated subcarriers this is called distributed style, while when occupying a set of adjacent subcarriers called localized. It is necessary to remark that, the additional FFT/IFFT blocks grow the complexity, particularly at the sender side, and hence moderate variations of the signal envelope are given by the massive computational processing.

1.2. Classical equalization schemes for multipath channels

In excellent communication systems, the received data is identical to one that is transmitted. Nevertheless, this is not the case for real communication systems, wherein wireless communication systems, the presence of natural and man-made objects made the

transmitted signals simultaneously travel over multi-paths to the receiver, each signal arriving along each path suffering from different attenuations and propagation delays. The resulting issue is the dispersion of the transmitted symbols. The multipath channel will generate ISI between symbols when the symbol period becomes shorter than the period of dispersion, which makes it very hard to reproduce the symbols at the receiver. Increasing the transmission rate and reliability is always one of the basic objects for the development of the wireless communication techniques. Furthermore, increasing the transmission rate reduces the duration of symbols compared to the delay spread so we have more ISI at the receiver. Accordingly, how to restore symbols damaged by ISI is an essential taks in wireless systems. To alleviate the harmful effects of ISI, equalization is generally used. A huge amount of research has been given to improve practical equalization techniques. Some traditional sorts of these techniques such as MLSE, LE, and DFE will be shortly demonstrated in what follows.

1.2.1. Linear equalization

Linear equalization (LE) attempts to suppress or minimizes ISI according to specific techniques, such as MMSE or ZF to yield an inverse of the channel so that the cascade of the channel and linear equalizer has a nearly flat response in the frequency domain. These two techniques are described in the sequel.

Zero Forcing (ZF) equalization attempts to eliminate all ISI from the observed signal. This is performed by the filter whose frequency response is precisely the inverse of the channel.

The frequency response of this equalizer is given by

$$f(\omega)_{zf} = \frac{1}{H(\omega)}, \tag{1.2}$$

where $H(\omega)$ denotes the channel's frequency response. As we can see, this filter can greatly remove all the channel effects, but enhances the variance of the output noise according to

$$\sigma_n^2 = \int_0^B \frac{N_o}{H(\omega)}\, d(\omega)\,. \tag{1.3}$$

By viewing this expression, it is clear to understand that if $H(\omega)$ is near zero, for an assigned spectrum of frequencies, the power of noise after equalizer is hugely enhanced. Furthermore, if $H(\omega)$ has a null than the ZF equalization becomes inefficient [19].

Due to the noise enhancement in ZF equalizers, different models that give an equilibrium between inverting the channel transfer function and retaining noise improvement, at a satisfactory level, have been suggested. One of them is the equalizer, the equalizer coefficients are estimated to minimize the mean squared error (MSE) between the transmitted data and the equalizer output [19] .The frequency response of this filter that reflects this rule is given by

$$f(\omega)_{mmse} = \frac{H^*(\omega)}{|H(\omega)|^2 + 1/SNR} \tag{1.4}$$

where SNR denotes the signal to noise power ratio. Obviously, the additional factor in the denominator to ensures that the noise power will be always finite at the output of the filter.

1.2.2. DFE system

In the situation, when the multipath communication channel makes drastic ISI distortion, the LE cannot yield adequate performance. Alternatively, A non-linear realization, named a decision feedback equalizer (DFE), is needed, particularly when deep spectral nulls occurred in the frequency response of the channel. The fundamental design of the DFE consists of feed-forward (FF) and feed-back (FB) filters. The DFE uses past corrected samples from a decision device to the FB filter and combines them with the FF filter output. In effect, the purpose of the FB filter is to subtract the ISI generated by the earlier recognized symbols from the estimates of the later samples [21].

DFE introduces error propagation effects because of incorrectly detected symbols that will increase rather than suppress the ISI, and may introduce more errors This is the most important drawbacks of DFE.

1.2.3. MLSE system

The optimum signal detection approach considers the detection of the whole sequence using the maximum likelihood criterion. The resulting maximum likelihood sequence estimation (MLSE) receiver yields optimum performance in terms of probability of error [20], [21]. MLSE uses the channel memory to find the most likely transmitted sequence. It does not increase the noise level. It has a computational complexity that increases exponentially with the length of the inter-symbol interference, which yields impractical equalizer. A more realistic MLSE would work on fewer symbols but still this can be computationally higher, in addition to tracking time-varying channels and can only create sequences with a notable time delay.

Generally, The configuration and implementation of these filters in the TD can be prohibitively complex and increase linearly with the channel's impulse response length, especially when the data rate becomes very high, where the symbol duration will be small relative to the channel length and the inter-symbol-interference spreads over hundreds of symbols [22]–[24].

Because the convolution in the TD becomes a multiplication in the FD and the complexity of the FFT\IFFT algorithm increases linearly with the logarithmic scale of the transmitted data length, which is usually more than the channel impulse response length, alternative solutions have been investigated by the transition of the equalization process from the TD to the FD. Hence, the equalization process can be carried out much easier.

1.3. Phase Noise in Oscillators

An oscillator is an autonomous electronic device, which produces periodic signals at specific frequencies. These periodic signals commonly used in digital electronic devices such as PCs to produce clock signals for timing and frequency synchronization operations, and carrier signals for passband transmission/reception and in processing wireless communications systems.

An excellent oscillator produces purely localized tones at the frequencies of interest to ideally fulfill the tasks of (up/down) conversions with the spectrum as shown in Fig1.6.

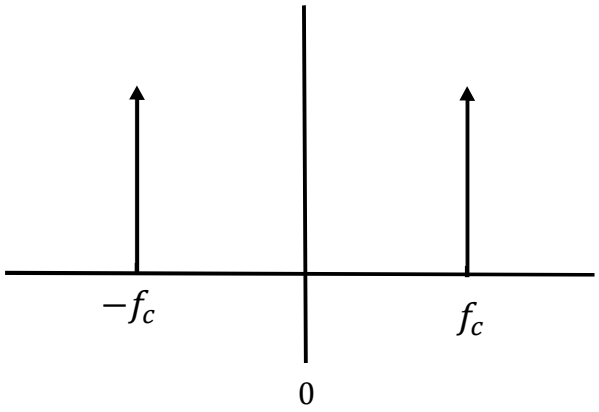

Figure 1.6: Ideal oscillator spectrum.

But in reality, the converting process is flawed, essentially due to the imperfections of the local oscillator (LO) devices that have been used in the communication transceivers. Practically, there are sidebands spectral spreading around the carrier frequency f_c, appearing high power levels at the nearby frequencies [25], as shown in Fig1.7. This spectral spread is mainly associated with physical quantities so-called random amplitude and phase instabilities [26] .

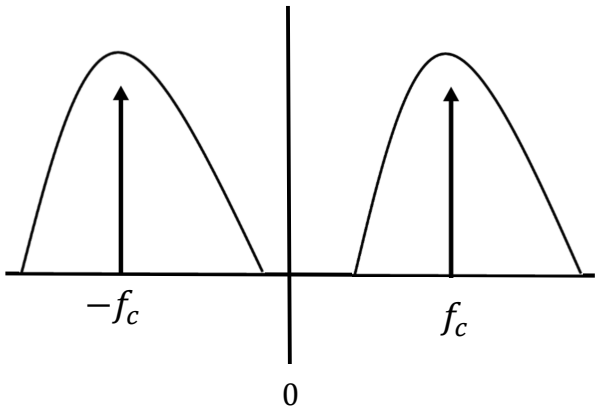

Figure 1.7: Spectral spreading in an oscillator.

In a well-designed oscillator, the amplitude is so stable and can usually be considered as a constant. There are usually two parts of the phase instability arising at the output spectrum of the LO. The first part produces discrete signals emerge as a separate

component at the non-integer multiples of the desired tones in the spectrum and they are referred to as spurious signals. The second continuous part seems as irregular (random) phase variations and is mentioned to as a phase noise (PHN). Fig1.8 show an example plot which includes PHN and a spurious signal.

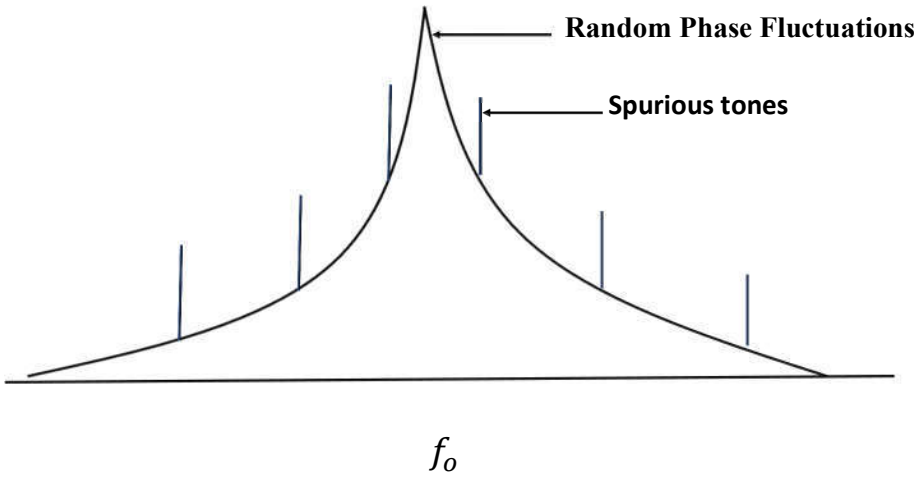

Figure 1.8: Spurious tones and PHN of LO phase instabilities.

The presence of random perturbation in the signal phase exhibits itself as a PHN in the FD and characterizes the frequency spectrum shape of the oscillator. PHN is a very important issue in the frequency generating systems because it can, for instance, increases the error rates in the digital system or corrupts neighboring channels and thereby limits the number of usable channels [27], [28].

Without PHN, the whole power of the LO would be concentrated at the frequency f_o. Nevertheless, the attendance of PHN spreads some of the power of the LO to the nearby frequencies, generating PHN sidebands, as shown in Fig1.9. This spectral shape is referred to as Lorentzian shape and f_m refers to the offset frequency from the center.

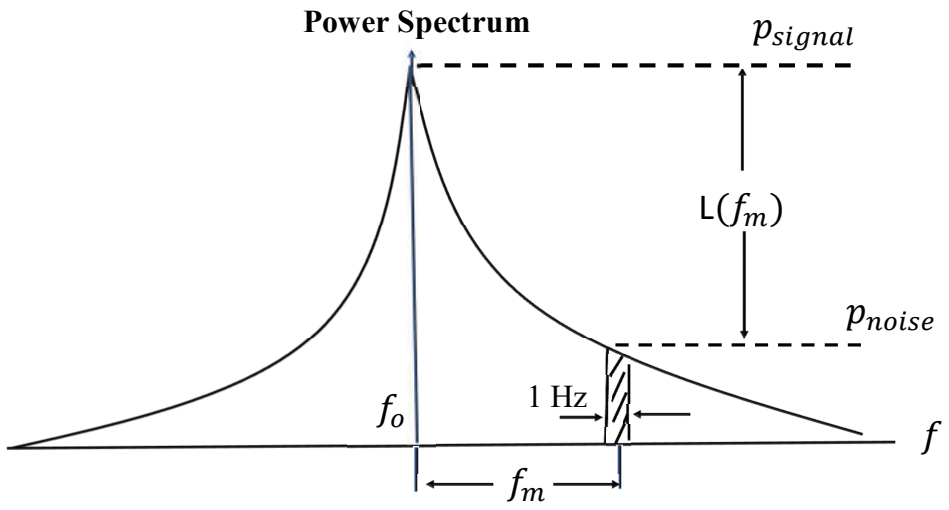

Figure 1.9: Phase noise SSB definition.

In [29], the PHN of a LO is typically quantified by the SSB power spectrum density, which is described as the ratio of the noise power, p_{noise}, in a 1 Hz BW at an offset f_m from the carrier frequency, to the signal power, p_{signal} , as shown in Fig.9 and is given by

$$L(f_m) = 10\ \log_{10}\left[\frac{p_{\text{noise}}\ (f_m.1)}{p_{\text{signal}}}\right]\ dBc/Hz \tag{1.5}$$

In summary, small quantities of noise in the LO can drive spectacular changes in the FD and TD properties. The influences of the PHN is the significant contributor to wasting the orthogonality between subcarriers and the rotation of the signal constellations which results in additional errors and therefore an excess in the bit-error-rate (BER) [30]–[32].

Therefore, PHN in wireless communication systems can be considered as one of the main performance limiters, that should be taken into considerations in system design.

1.3.1. PHN Modeling

1.3.1.1. Phase locked loop Oscillator Model

Most of the communication systems widely utilize some form of the feedback mechanisms, called phase locked loop (PLL) as a frequency generator. Due to its stability and controllability. The PLL generates a broad range of frequencies and phase locked (bounded phase drift) to a reference higher quality oscillator.

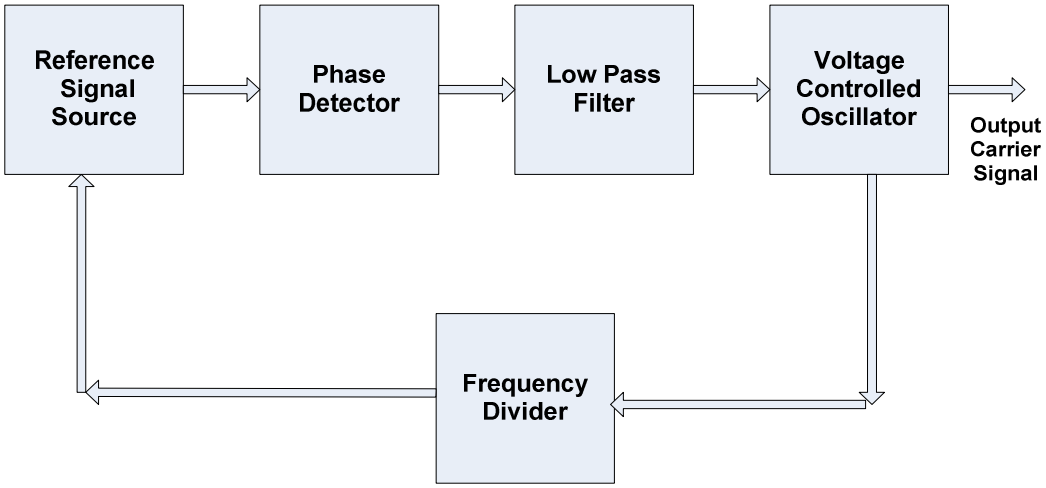

Figure 1.10: The schematic diagram of PLL frequency generator.

As shown in Fig1.10 generally, the major components of the PLL include a frequency divider, reference signal source, phase detector, LPF and VCO. The phase detector compares the phase of the signals of both reference oscillator and output, and generates an error voltage signal filtered by low pass filter and then is used to drive the VCO which generates the output frequency comparable to the voltage at its input. The error signal will grow when the output frequency drifts from the reference input and running the VCO frequency in the reverse direction to reduce the error, therefore the PLL is said to be locked.

Each component in the PLL schematic diagram can be considered as a source of noise and should be taken in concern when driving the output spectrum of the PHN as shown in Fig1.11 from [33].

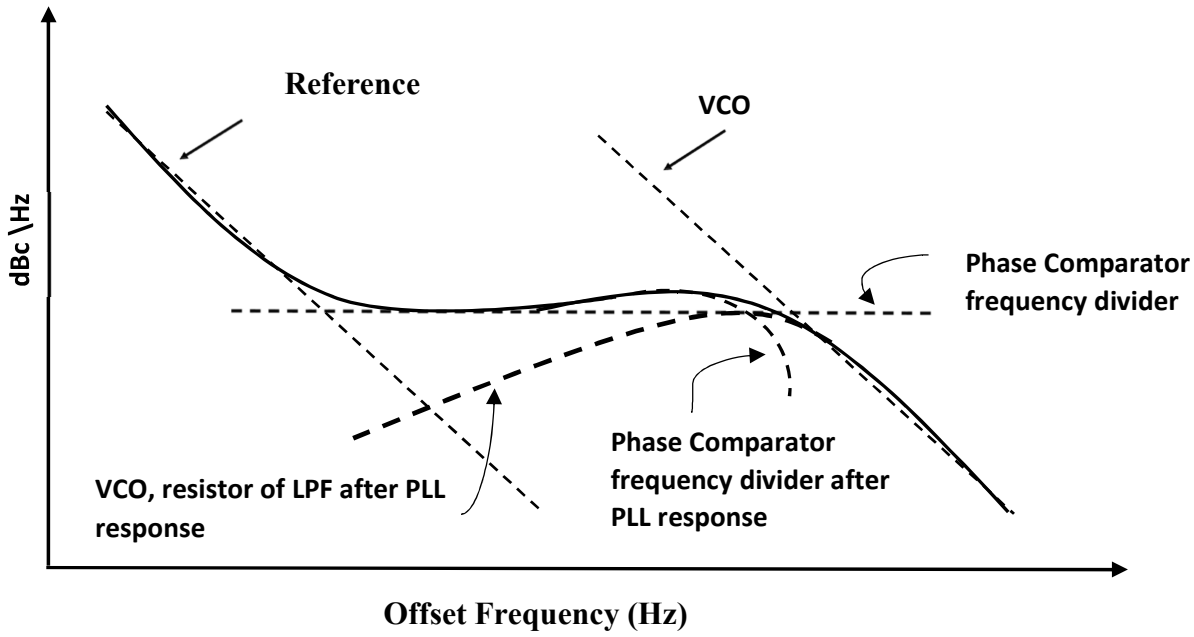

Figure 1. 11: Contributions of various sources toward PHN spectrum.

By considering the white sources of noise (like shot and thermal noise), and the PLL in a locked state, the authors in [34] showed that the resulting PHN in the PLL-device is a stationary Gaussian process and adopted in the IEEE standards, e.g. 802.11g.

1.3.1.2. Free running oscillator model

The phase of the free-running oscillator (FRO) grows and drifts freely (unbounded). In many practical applications FRO is stabilized inside a PLL. We can consider that PHN of the FRO has the strongest influence on the PLL output [35], [36] .

For white noise sources, the FRO models the phase noise effect by a simple mathematical random realization called Brownian motion or Wiener process whose variance increases linearly with time and with PSD that follows a Lorentzian shape [37].

Oscillator PHN arises from various sources of noise inside the electronics. These sources can be classified as white (like Shot and thermal noise) and colored noise (like supply-noise, burst and 1/f flicker noise). A white noise process has a flat PSD, which isn't the case for the colored noise. Figure 1.12 presents a typical PSD of the noise sources inside the LO electronics [35], [38]. These noise sources cause short-term instabilities, which typically last for few seconds.

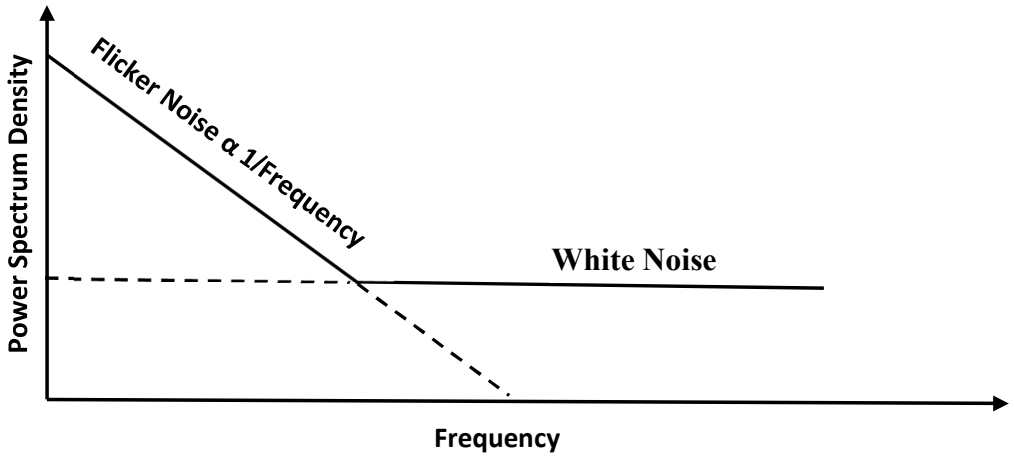

Figure 1.12: PSD of noise inside the LO electronics.

For simplicity, PHN will be modelled utilizing the Free-Running Oscillator (FRO) model, while more realistic and complex PLL PHN model will be left out from this thesis.

1.4. Thesis objectives

Based on the aforementioned discussion, this thesis presents respective studies around the combined FD equalization and PHN mitigation.

The objectives of this thesis are:

- An exhaustive to literature study the equalization in the frequency domain.
- A novel joint SC-FDMA FD-E and PHN compensation scheme is adopted in the FD as a single process to the frequency domain equalizer.
- Based on the reliability of the feedback symbols improve the equalization process by overcoming the dilemma of error propagation.

1.5. Organization of the thesis

This thesis comprises five chapters. Chapter 1 give a brief introduction to subject matter. Chapter 2 will be devoted to the literature review pertaining to this research work, mainly to frequency domain equalization and phase noise in an OFDM and SC-FDMA systems. In chapter 3, a novel joint architecture for frequency domain equalization and PHN compensation is proposed and tested. Chapter 4 treats the same problems as that in chapter 3 with a different approach and this is by using a reliability test. Finally, chapter 5 summaries this work and highlights some potential research in the context of frequency domain equalization and PHN compensation.

CHAPTER 2

LITERATURE REVIEW

2.1. Frequency domain equalization

In recent years, pay attention to the wireless channels has been increased quickly. The multipath nature of the wireless communication channels gets difficulties to recover the fast-transmitted data at the receiver side due to the huge amount of the produced inter-symbol interference (ISI) among the transmitted symbols. Consequently, how to overcome inter-symbol interference problem is an essential challenge for the wireless communications systems. To mitigate the detrimental effects of ISI, powerful equalization strategies inevitable. A huge amount of research has been given to improve the practical equalization techniques in the time domain. The configuration and implementation of these techniques can be prohibitively complex when the data rate becomes very high, where inter-symbol-interference spreads over hundreds of symbols. The complexity of the computational rises quadratically with the bit rate for the classical time domain equalization TD-E schemes [20], [39], [40].

Because the convolution in the TD becomes a multiplication in the FD, alternative solutions have been investigated by the transition of the equalization process from the TD to the FD. Hence, the equalization process can be carried out much easier with payment for equalization rises somewhat more than linear with the bit rate.

In OFDM, a block of M data symbols at the transmitter side, by IFFT processing, multiple Narrow bandwidths modulated sub-carriers are transmitted in parallel. The reverse operation will be carried at the receiver side by FFT operation to extract the

transmitted symbols. The length M of the collected data block should at least be fourfold larger than the maximum length of the channel to reduce a portion of the cost, resulting from the addition of cyclic prefix (CP) at the start of each block. CP involves a copy of the final symbols of the block, with a period greater than the maximum period of the channel. CP Limits ISI of each block from its former and shows the received block to be cyclic with cycle M, this allows the emergence of the circular convolution which is the basic function to allow FFT and FD-E work properly [3].

The multiplications number per data symbol needed for TD-E proportional to the maximum length of the channel while $log_2 M$ multiplications per data symbol needed for OFDM, including all the transceiver operations. Therefore, OFDM seems to give a reliable performance and complexity than traditional SC-TD-E for a large multipath spread, where M proportional to the maximum length of the channel [41]. In channels with critical delay spread when the SC system sends the modulated signal at a high symbol rate, the FD-E is computationally modest than its corresponding classical linear TD-E for the identical judgment OFDM is modest, where the equalization is done on a block of length M at a time. A SC style including FD-E has approximately an identical performance and computational complexity as an OFDM, even for a very long channel [41], [42].

As it has been mentioned earlier, the lower PAPR is the primary contribution of SC-FDMA over the OFDMA which allows the MS to be more efficient in the power transmission. Therefore, SC-FDMA has been utilized in the LTE-UL wireless communication systems [43]. Additionally, SC-FDMA with extra adaptability in resource allocation, may be viewed as a multiple access technique of the SC-FDE [18].

Consequently, All the equalization algorithms for the SC-FDE may be deployed in SC-FDMA due to its single-carrier nature.

2.1.1. A hybrid-DFE scheme

LE provides bad performance than the DFE due to its noise enhancement problem, which may result in large performance degradation especially in the case of deep frequency-selective fading. DFE provides optimal SC-E algorithm due to its strength to remove post-cursor-ISI utilizing earlier recognized symbols [20]. In conventional TD-DFE equalizer, both feedforward (FF) and feedback (FB) filters are implemented in the TD. Filtered symbols are used to eliminate their interference impact from the subsequently detected symbols.

A hybrid-DFE strategy in SC-FDE was examined in [44], using a feedforward filter in the FD and feedback filter in the TD. In [44] , it was shown a H-DFE enables reaching an equal performance gain as a high rate coding scheme, with notable and smaller configuration efforts. Also, Huang et al [45] extended the design of the H-DFE from SC-FDE to SC-FDMA.

The H-DFE for SC-FDMA receiver combine the FD-feedforward,G_{FF}, and TD-feedback, g_{FB}, filters Fig. 2.1 depicts this structure. Also, as shown in this figure $\hat{x}_m$ indicates the hard-decision (HD) feedback symbols, and $\tilde{x}_m$ indicates the feedback equalized symbols. This paper shows the ability to eliminate earlier echoes ISI, which make the H-DFE results in an excellent performance than LE.

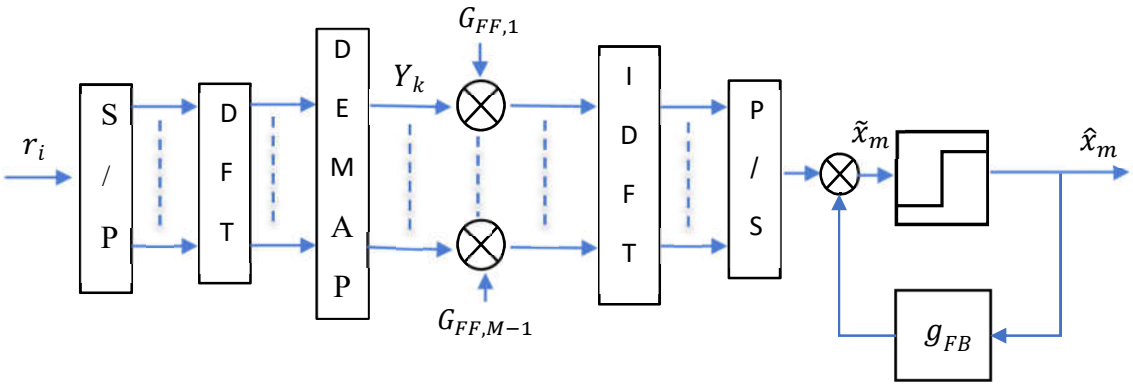

Figure 2.1: Structure of H-DFE system.

The H-DFE equalizer need matrix inversion operations in order depends on the number of taps in the TD feedback filter, which has the significant impact on the obtainable equalization performance.

2.1.2. Totally FD-DFE scheme

Zhang et al [42] developed a new SC-FDMA FD-DFE equalization approach for all subcarrier mapping schemes such as localized or distributed allocation, where the feedforward and feedback filters are handled in the FD through FFT and IFFT operations as shown in Fig. 2.2.

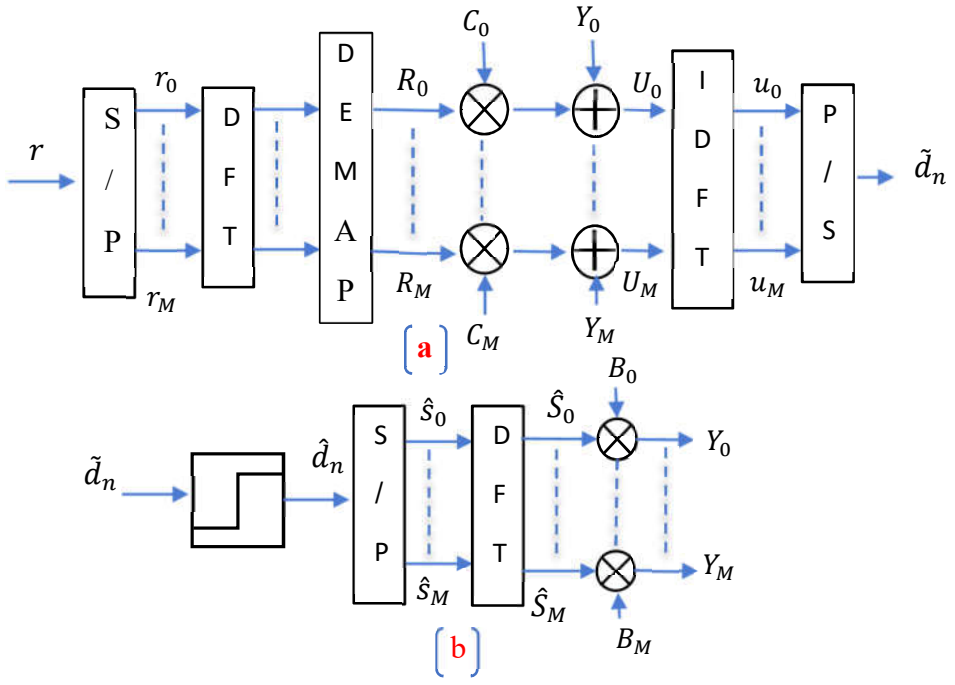

Figure 2.2: Structure of FD-DFE system.

2.1.3. Iterative FD-DFE scheme

An iterative FD-DFE for SC-FDE, in which both the feedforward and feedback filters work in the FD by applying FFT and IFFT procedures was developed in [17][46] and is shown in Fig.2.3. The matrix inversion needed in the H-DFE is thus excluded. The equalizer requires the calculation of the two filters (feedforward and feedback) coefficients at each iteration. In addition to, the estimation of some system parameters each iteration like the correlation between the transmitted and the detected symbols, which increased the computational complexity of the system. Unlike the former I-FD-DFE the authors in [47] calculate the equalizers coefficients only once without the need for updating at each iteration, consequently, a significant decrease in the computational complexity is obtained.

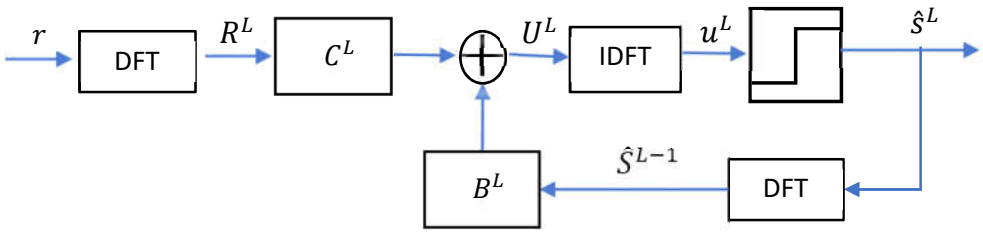

Figure 2.3: Structure of I-FD-DFE system.

In our work, we will extend the implementation of the iterative frequency domain DFE (I-FD-DFE) in SC-FDMA. Since growing the complexity at the BS is applicable, SC-FDMA with H-DFE or FD-DFE or I-FD-DFE can be recommended for UL in an LTE system specifically when the channel is in deep fading, this gives the ability to gain efficient power transmission. The derivation of the coefficients of the FD-LE or FD-DFE can be obtained by the MMSE criterion as in [41] or by using adaptation algorithms like LMS or RLS techniques as in [13][48].

2.2. Phase noise

One of the principal RF impairments that generate shifts of the transmitter and receiver oscillators signals, and emerging from errors in the fabrication process of the LO, is a random process called phase noise (PHN). PHN influences must be accurately analyzed and examined when creating standard wireless communication systems because a reliable forecasting of the tolerable PHN can enable wireless system designers to relax specifications.

2.2.1. PHN in OFDM system

PHN influences and degradations entered in OFDM system have been examined by various authors in the literature [49]-[65]. The theoretical analysis has been

identified two distinct sorts of impacts that are submitted by PHN in OFDM signals, common phase error (CPE), zero frequency component of the PHN, which rotates each demodulated symbol by the angle that's proportional to the average phase variation inside a single OFDM symbol and inter-carrier interference (ICI), which generated by PHN non-zero frequency components. ICI added like AWGN.

The authors of [49], [50] noted that the CPE, which is attached to every sub-carrier is equivalent to the data inside it and multiplied by the average of the PHN over all the other sub-carriers. CPE causes rotation of the constellation and fixed for all sub-carriers. They have used pilot-based channel estimation, as a way to combat both channel and PHN influences collectively, particularly when the PHN bandwidth is smaller than the OFDM subcarrier spacing. At this condition, the CPE dominate the ICI and can be fixed by simple phase de-rotation. If the PHN bandwidth is more than the OFDM subcarrier spacing, the conventional fixing way cannot cope with the CPE and the fixed signal can show an even poorer SER than the unfixed one. Also, these papers investigated the impact of the sub-carrier bandwidth on the PHN error fixing facilities, where increasing the number of sub-carriers reduces the sub-carrier bandwidth against PHN bandwidth, and the fixing may be worse in this case as we mentioned previously.

In [51], depending on the PHN variance, the authors investigated the SNR degradation ($degr_{SNR}$) produced by the PHN in OFDM. The deterioration is extremely higher, particularly in the scheme infected by PHN with great variance, and the total PHN power spectrum necessity lowered in the region of the spectrum near to the

carrier (lowering PHN variance) or utilizing a suitable PHN fixing scheme that enables the LO's specifications to be significantly relaxed to reach a satisfactory performance.

However, the authors of [52], [53] examined the influences of PHN on coded OFDM where the entering bitstream is coded utilizing BICM then transmitted over frequency selective channels. From the information theoretic perspective, they have chosen the capacity and cut-off rate to characterize system performance. Capacity is the final limit can be achieved for the system rate while the cut-off rate is the attainable rate when a finite complexity coding design is handled. As $\frac{\Delta f_{3dB}}{\Delta f_{car}}$ raises the cut-off rate and capacity drops, this is the result of the increasing ICI term. Additionally, for a given value of $\frac{\Delta f_{3dB}}{\Delta f_{car}}$ the OFDM scheme performance becomes very sensible to PHN, particularly when higher modulation order is employed, meaning that modulations by utilizing high-order constellation in a wireless system can be restricted by PHN presence. Moreover, handling an interleaving depth over some tens of OFDM data symbols forming the PHN features almost comparable to AWGN.

Rave et al [54], formed the up/down conversion LO as a FRO and put all the defects on the receiver side. PHN in the case of the FRO, modelled as a Wiener process, has variance that increases linearly with time at rate c depends on the LO nature. Accordingly, the constant c suffices to effectively describe the PHN process. In reality, c isn't instantly accessible. Alternatively, a model that utilized to define the LO performance is the SSB LO PSD functions $L(f_m)$[dBc/Hz] where f_m is the frequency offset with regard to f_o. The link among $L(f_m)$ and c is obtained by Δf_{3dB} BW of $L(f_m)$. Δf_{3dB} can be taken from the determined data of $L(f_m)$ which is generally obtainable

and c can later be determined from Δf_{3dB} as $c = \frac{\Delta f_{3dB}}{\pi f_o^2}$, the LO carrier frequency indicated by f_o [55].

PHN suppressing in OFDM systems can be described as receiving adequate knowledge of the PHN waveform as possible. Once we have this knowledge we can utilize it to mitigate the PHN influence. The simplest method will be to approach PHN with fixed value, i.e., its average. Unconventional methods to get useful approaches of PHN is to attempt to predict its higher spectral components.

Rave et al. [54] proposed ICI cancellation algorithm, where the official procedures for performance enhancement were to estimate the CPE and compensate its impacts. This was done by just de-rotating the constellation in the FD, which is similar to approaching the PHN inside one OFDM sub-carriers block with its zero-frequency spectral component. CPE is the highest harming error, that generates constellation rotation and impacts all symbols in a similar manner and can be interpreted as a regular PHN error. Furthermore, the ICI error element appears as an AWGN noise which produces irregular and nonsystematic errors. The existence of ICI depends on the amounts of phase divergence from its average value inside one OFDM symbol. The AWGN noise term will collectively, with the ICI PHN element describe the measuring noise which influences the characteristic of the estimation process. As a result, an algorithm to fix the CPE will regularly be restricted only to eliminate some portion of the errors. To continue this regularity the ICI should be counted also as a corruption factor. Here, authors utilize the very small low-pass nature of the PHN bandwidth contrasted with the sub-carrier bandwidth to drive the algorithm to cancel the ICI.

The more spectral components (DFT coefficients) of one PHN random realization, the greater the approaching of the PHN waveform. PHN spectrum nature makes it possible to utilize few numbers of the low-pass frequency components to give the good estimation of its shape. Consequently, identifying a lot of DFT coefficients of the PHN allows the probability to approach the PHN shape to the higher order than simple approximation with its Zero-frequency component and yields a much mitigation of it. Initially, they made OFDM demodulation, CPE estimation, correct the demodulated signal by de-rotation, use such de-rotated signal and made the hard decision, use these hard decisions and perform DFT coefficients estimation by using the MMSE criteria. The estimated DFT coefficients are used to generate PHN waveform approaching. The nature of the suggested ICI removal algorithm should give estimates of several spectral components as possible to increase the performance of the cancellation.

Petrovic et al. [56] , based on the statistics of the PHN, denoted the state space model of the system to enhance the estimation process. The algorithm utilized pilot based method in the FD and extended Kalman filter (EKF) to obtain the MMSE estimate of the state, which is the average deviation of the PHN CPE. The impact of ICI on the system's performance becomes higher, as the PHN bandwidth Δf_{3dB} increases producing an error floor with high symbol error rates and degradation in the performance of the algorithm.

A closed form formulation for the correlation matrix of the DFT coefficients of PHN was derived in [57]. The entire ICI power equals the total summation of the

diagonal components of the correlation matrix. The performance of the ICI mitigation algorithm influenced by both PHN properties and the channel profile. Understanding ICI is really an important problem and the statistical characterization of the ICI term is considered so far to be Gaussian. But the authors in [57] observed that the Gaussian assumption of ICI distribution didn't hold and has influences on the system's performance. In AWGN channels, they observed that the largest amount of interference emerged from adjacent subcarriers and concentrated around the zero-frequency component as a result of the Lorentzian spectrum. While in the frequency selective channel the spectrum of the PHN forming by the channel, so notable ICI component can come from very far sub-carriers. Hence, very small components of PHN can hold a very notable contribution to the ICI as a result of the channel characteristics. This illustrates why we want large amounts of PHN DFT coefficients to enhance the algorithm performance.

Fettweis et al. [58] suggested an iterative PHN Suppression algorithm based on the algorithm in [54], where the spectral coefficients of PHN have been used to improve the mitigation process. After initial CPE improvement, the incorrectly recognized symbols, which are supplied to the MMSE estimator to estimate PHN DFT coefficients, will have a critical impact on the estimation method, particularly when the PHN bandwidth becomes larger, consequently a large ICI, which affects the estimation of the CPE also. The reduction of the fed back falsely detected symbols will enhance the characteristic quality of the PHN estimation and suppression. To enhance the performance of PHN suppression by reducing the error propagation, the iterative approach has been considered. After the first iteration of the algorithm [54],

the estimated symbols are utilized to enhance the estimate of the DFT coefficients, where the demodulated QAM symbols feedback again to the Step of DFT coefficients estimation and suppression. This means, reconstructing the transmitted symbols after PHN correction and use them repeatedly for a continuous PHN estimation and compensation.

Also, the iterative strategy of PHN suppression and decision feedback errors minimization has been presented in [59] by utilizing an APP decoder that provides soft or fidelity information that in turn is utilized to pick the greatly reliable symbols for Bayesian estimation of the DFT elements of the PHN single realization up to a certain order. In [32], the authors based on [54] extended the iterative PHN estimation and suppression algorithm to the receiver with PLL. PLL separates the low-frequency component of PHN, which produces easier CPE correction mechanism and gives an excellent start for ICI reduction.

Songping et al. [60] suggested a different and easy PHN-S algorithm especially for IEEE 802.11a standard, that owns an excellent performance when dealing with PHN. This algorithm uses the benefit of the pilot and null samples given in IEEE 802.11a standard, to estimate the zero-frequency component of phase noise by least-squares (LS) and ICI plus noise energy, respectively, then use them to calculate the MMSE equalizer coefficients to get the transmitted data samples after equalization. After that, decision feedback for the estimated signals is used to update the estimate of the zero-frequency component instead of pilot samples and repeat the equalization again until all symbols have been processed. It was shown that this algorithm holds

significantly excellent performance than other algorithms while maintaining minimal computational complexity and successfully suppresses PHN. The impact and mitigation of PHN on OFDM have been extensively analyzed in [61]-[65] and references therein.

2.2.2. PHN in SC-FDMA system

SC-FDMA is extremely vulnerable to PHN, despite it holds a moderate PAPER in comparison to OFDMA. It acquires the vulnerability to the transceiver defects from the OFDMA.

In both cases, OFDMA and SC-FDMA, the CPE is clearly the same. Regular rotation caused by the zero-frequency component of the PHN, that all modulated symbols inside one OFDMA or SC-FDMA block experiences. Other terms produced by the spread of the power of all of the neighboring subcarriers on top of each other is extremely diverse. In OFDMA, the additive ICI impact follows the impact of AWGN. The impacts in SC-FDMA are also comparable; however, it isn't identical. This is called user self-interference. In the beginning, the modulated symbols of each user are one by one attenuated and rotated by every spectral component of the PHN. The whole effect, hence, depends on the modulated symbol of each user and every spectral component of the PHN. Consequently, the whole impact of the attenuated demodulated symbols is an almost extra rotation that is changed for each symbol. Furthermore, there is an extra impact similar ICI in OFDMA called inter-user interference (IUI). As the number of users grows, the additive influence starts to follow more and more the ICI influence that the OFDMA holds. This is because the IUI

goes great when the user's numbers increase, however, when a few numbers of users are present, the U-SI become the strongest additive effect.

Syrjala et al. [66] submit based on some of the OFDMA-estimation algorithms in the literature a new practical approach to alleviate PHN and understand its effects in SC-FDMA systems. Initially, the transmitted symbols are detected after equalization and CPE mitigation. The principal dilemma that remains is the reduction of the additive effects of IUI and SUI. The principle idea of the algorithm based on the regeneration of the received signal from the recognized symbols, considering that, they were the ones transmitted. The regenerated signal is currently, almost the received one without PHN. Hence, when the received signal with PHN divided by the restored one, the resulting signal is an almost the only distinction among the regenerated and the received signals, which is the PHN in the excellent situation. Then the algorithm takes the DFT of the estimated PHN and takes a few of the centermost frequency elements to alleviate PHN according to [55]. After removing the additive effects of the PHN and obtaining the new detected symbols, the newly detected symbols can be used again to estimate the PHN. Therefore, the mitigation may be utilized iteratively. The complexity of the mitigation depends on the DFT components used in the algorithm. The algorithm is based on the fundamental concepts of PHN reduction algorithms for OFDMA [32] and [67].

Ryu et al.[68] studied the influences of PHN in the LO and back-off at the HPA which may be the dilemma for the UL. Also, proposed the equalizer of an excellent PHN suppression algorithm based on the FD-E method and block type pilot to exclude ICI part efficiently. This is logical hypothesis through the pilot SC-FDMA, but since PHN is a quickly varying process, it isn't effective in general.

Zhang et al.[69] have analyzed SC-SFBC to decrease the PAPR of the MIMO SC-FDMA signal, where the Alamouti SFBC design used in the traditional MIMO scheme, shape the signal spectrum and break the SC feature and rise the PAPR. CFO and PHN are very challenging difficulties in SC-FDMA scheme, so the authors recommended a block-type pilot-based common algorithm to overcome the ICI generated by both CFO and PHN rather than estimating both CFO and PHN by two different algorithms. The recommended algorithm immediately estimates the interference components together with a common algorithm. Therefore, it can decrease the complexity and avoid the interactions between estimating CFO and PHN.

The direct conversion (DC) transceiver faces different dilemmas, emerging from the defects and errors, accompanying the invention process such as CFO and PHN. The authors in [70] determine an analytical formulation of the EVM for MU SC-FDMA UL transmissions. EVM is broadly utilized in most of the future wireless systems as a performance metric. Besides, based on the determined EVM definition, they distinguish the performances of both localized and distributed subcarrier mapping methods and the resistance to both PHN and CFO. In localized mapping scheme, each user is designated a set of adjacent sub-carriers, while in distributed mapping, the users are designated separated sub-carriers over the transmission bandwidth. CFO and PHN produce a flow of the energy of each sub-carrier into its adjacent, and this is apparent in the arrangement of the corresponding FD circulant matrices. These matrices are banded with greatest of the energy collected in some off-diagonals nearby the central diagonal. Therefore, most of the interference power affecting the k^{th} user sub-carriers flow from the adjacent sub-carriers

which relate to the same user and other users in the localized and distributed sub-carrier mapping methods, respectively. In other words, CFO and PHN produce SI and IUI to the k^{th} user in the localized and distributed mapping schemes, respectively. Based on the mathematical results they believe that the generated IUI is more critical than the generated SI. Accordingly, the localized mapping is more resistant to CFO and PHN than the distributed.

The interleaved SC-FDMA, under excellent conditions, out-performs the localized SC-FDMA by employing the frequency diversity. While in the attendance of PHN, localized SC-FDMA is more resistance to PHN than interleaved SC-FDMA, which implies that the overall interference occurring due to PHN is conditional on the sub-carrier mapping scheme.

Sridharan et al. [71] explain how the performance change depending on subcarrier mapping scheme, if it is interleaved or localized, through the examination of the SINR definition in the two situations. SINR in the state of interleaved SC-FDMA is very detrimental than that for localized SC-FDMA, this decline in SINR results essentially because of the change in the variance of MUI (interference occurring from data streams corresponding to other users) for the two situations. At high SNR, when the channel coefficients become independent, the variance of the MUI becomes extremely large, therefore it is logical to believe that irrespective of sub-carrier allocation scheme, MUI is likely to dominate over SI (interference inside a user's data stream). In the case of localized SC-FDMA, the important frequency components that hold most of the energy of the PHN are included in the SI while in the case of interleaved SC-FDMA included in MUI. Therefore, localized SC-FDMA is more resistance to PHN than interleaved SC-FDMA.

Recently, millimeter-wave (mmWave) communications has gained a great attention in the Fifth Generation (5G) cellular networks due to the availability of wide spectrum at higher gigahertz frequencies [72]-[73]. Since the frequency of mmWave is extremely high, PHN greatly deteriorates the transmission performance. The authors in [74], find an effective method to tackle the PHN influences in the mmWave single carrier frequency domain equalization in a multiple-inputs-multiple-output (SC-FDE MIMO) system, by using a modified version of the decision-directed phase noise compensation (DD-PNC) algorithm proposed in [75] for single input and single output (SISO) system. DD-PNC estimates the PHN at each sampling time by using one tap least mean square (LMS) algorithm by utilizing the outputs of the decision as a reference signal.

At the end, we can summaries the literature as follow , many authors studied the effect of PHN in OFDM as [51] and [55] . Also, many authors provided simple PHN compensation (CPE compensation) as in [49], [50],[53] and [54]. Additionally, many authors provided CPE and ICI compensation by the estimation of the PHN DFT coefficients as [54] [56] and [57]. Also, many authors suggested iterative PHN suppression algorithms as [58], [59] and [60] based on the estimation of the PHN DFT coefficients iteratively after the CPE Suppression. Moreover, many authors studied the effect of PHN in SC-FDMA as [68] [66][69] [71] and [70], one of them [66] provided an iterative PHN compensation algorithm.

CHAPTER 3

SC-FDMA FREQUENCY DOMAIN EQUALIZATION AND PHASE NOISE COMPENSATION

A Discrete Fourier transform (DFT) precoded OFDM scheme called the Single-Carrier-FDMA (SC-FDMA) is an excellent design that has been adopted for uplink transmission in the LTE standard [77]. The presence of local oscillator impairments (phase noise) and bad environment (deep fading) have deleterious effects on the performance of the SC-FDMA system, if not taken into account. In this chapter, we propose a new approach to mitigate both of the PHN and the deep fading effects in the SC-FDMA system iteratively. This is achieved by exploiting the nature of the PHN in both time and frequency domains in addition to the iterative nature of the frequency domain equalization algorithm.

3.1. Introduction

Over the last few years, the demand for broadband wireless communication services was the most probable goal for all customers. This demand has brought much attention to new wireless technologies which support high data rate transmission and immunity to Radio Frequency (RF) impairments. Multi-carrier (MC) Orthogonal frequency division multiple access (OFDMA) schemes became within the past few years the dominating principle for broadband wireless applications because of their high spectral efficiency obtained by selecting a special set of overlapped orthogonal subcarriers and their robustness against selectivity of the channel [1].

Despite the benefits of OFDMA, it still suffers from several drawbacks , for example high peak-to-average power ratio (PAPR) that results in low power efficiency at the mobile

units [76]. To alleviate the high PAPR problem a modified form of OFDMA was investigated and called single carrier FDMA (SC-FDMA). SC-FDMA utilizes SC modulation and frequency domain equalization (FDE). Also, it has a similar performance and complexity as that of the OFDMA with low PAPR. Since then, it has been adopted for uplink transmission in the LTE standard [77]. For this purpose, a variety of equalization mechanisms were proposed over the last few years to mitigate inter-symbol interference (ISI) in fading channels. The configuration and implementation of these filters can be prohibitively complex when the data rate becomes very high, where the inter-symbol-interference spreads over hundreds of symbols [39][78][79].

Because the convolution in the time domain (TD) becomes a multiplication in the frequency domain (FD) it was found that FD-DFE is now attractive when dealing with deep fading scenarios due to its strength to remove post-cursor- ISI by utilizing earlier recognized symbols and affording less noise enhancement [78]. In conventional DFE equalizers, fed back filtered symbol decisions are used to eliminate their interference impact from subsequently detected symbols. In [42], the implementation of the H-DFE to SC-FDMA was investigated where the feed-forward (FF) filter was implemented in the TD while the feed-back (FB) in the FD. In [45] , both filters were implemented in the FD. However, both FD-H-DFE & FD-DFE improve the FD linear equalization process, their error propagation, arising from feedback incorrect decisions in low SNR, will become more serious especially in deep fading.

To alleviate this error propagation effect, many algorithms have been proposed such as [80][81][82]. In[17],[46], an iterative FD-DFE was studied, in which both the feedforward and feedback filters operate in the FD. Iterative-DFE provides good

performance in deep fading where the error propagation will be restricted to only one block of the transmitted data.

One of the principal RF impairments generate shifts of the receiver and transmitter oscillators signals and emerging from errors in the fabrication process of the LO, is a random process called phase noise (PHN). PHN influences and degradation entered in OFDM systems have been examined by various authors [50][51][52][83]where many ways to combat PHN have been proposed. Inserting pilots in SC-FDMA block is a waste of bandwidth, therefore, tracking of PHN is very difficult. In [84], a high complex non-pilot PHN estimation mechanism applicable only to BPSK and QPSK modulation schemes has been derived. The authors in [85] proposed a separate compensation mechanism iteratively for both transmitter and receiver PHN without utilizing its low-pass property. The low-pass nature in the FD and its smooth variation from one symbol to the next will be utilized here in our work. The details of this design will be details later after a brief description of the system's model.

3.2. System Model

3.2.1. SC-FDMA

Figure 3.1 shows the structure of SC-FDMA system. We consider a system with N_u users and subcarriers $M = N \times N_u$, where each N subcarriers assigned to only one user either in localized mode or distributed mapping mode after the N-point FFT transformation. Then after M-point IFFT a cyclic prefix with length L_{cp} equal to or greater than the channel's impulse response length, L_{ch}, will be inserted.

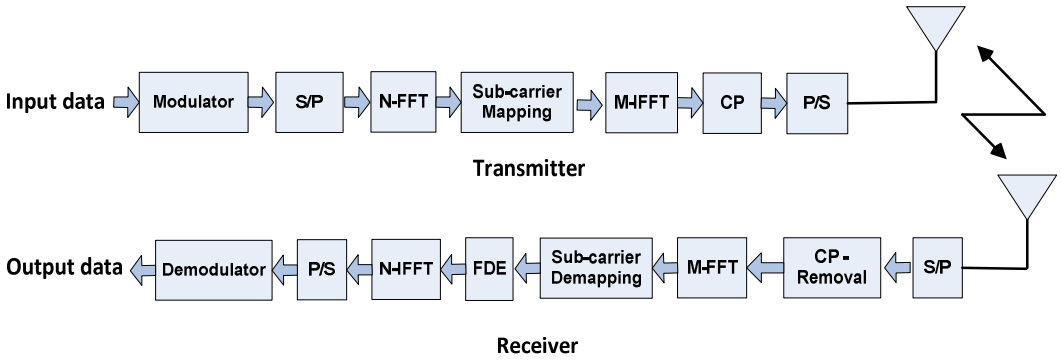

Figure 3.1: SC-FDMA system diagram.

The time domain transmitted vector corresponding to the K^{th}user without the cyclic prefix can be written as

$$g_k = F_M^H T_k F_N s_k \,, \tag{3.1}$$

where T_k is an $M \times N$ sub-carrier mapping matrix, s_k is an $N \times 1$ symbol vector of the K^{th}user, and $F_N \; and \; F_M^H$ are the FFT and IFFT matrices with dimensions $N \times N$ and $M \times M$, respectively. Assuming h_k is the $(L_{ch} \times 1)$ impulse response of the channel between the K^{th}user and the base station (BS) with max delay spread L_{ch} shorter than the cyclic prefix to completely eliminate the ISI. The opposite procedures will be done in the receiver side. The cyclic prefix addition on the transmitter, and elimination at the receiver converting the linear convolution with the channel to circular.

The time domain received signals corresponding to all N_u users for t^{th} SC-FDMA symbol can be given by

$$r^t = \sum_{l=0}^{N_u-1} H_l^t \, g_l^t + n^t, \tag{3.2}$$

where H_l^{th} is the $(M \times M)$ channel circular convolution matrix with first column comprises the impulse response of the channel between the l^{th} user and the BS and n^t is the $M \times 1$ AWGN with variance σ_n^2.

After M-FFT transformation, the frequency domain received signal is given by

$$R^t = F_M\, r^t = \sum_{l=0}^{N_u-1} F_M H_l^t\, g_l^t + F_M\, n^t. \tag{3.3}$$

To simplify the derivation, we will release the symbol index,

$$R = \sum_{l=0}^{N_u-1} \widehat{H}_l\, T_k F_N s_k + F_M\, n\,, \tag{3.4}$$

where $F_M H_l F_M^H = diag\big(FFT(h_l)\big) = \widehat{H_l}$.

After demapping the FD received signal for k^{th} user is given by

$$T_k^H R = T_k^H \textstyle\sum_{l=0}^{N_u-1} \widehat{H}_l\, T_k F_N s_k + T_k^H F_M\, n\,. \tag{3.5}$$

Due to the orthogonality property of the mapping matrix

$$T_k^H T_l = \begin{cases} I_N, & k = l \\ 0_N, & k \neq l \end{cases}$$

the FD received signal for k^{th} user is given by

$$R_k = T_k^H \widehat{H}_k T_k F_N s_k + T_k^H F_M\, n\,,$$

$$R_k = \widehat{\overline{H}}_k F_N s_k + T_k^H F_M\, n\,, \tag{3.6}$$

where $\bar{\hat{H}}_k = T_k^H \hat{H}_k T_k$ is a $(N \times N)$ sub-matrix of $(M \times M)$ $\hat{H}_k$ matrix. Consequently, the received signal in terms of the b^{th} frequency bin can be written as

$$R_{k,b} = \bar{\hat{H}}_{k,b} S_{k,b} + N_b \,, \qquad \text{where } b = 0,1, \ldots \ldots, N-1. \tag{3.7}$$

3.2.2. Frequency Domain Equalization

As it known the linear equalization for deep fading channel may amplify the noise at the spectral null which deteriorates the SC-FDMA performance in the time domain, DFE effectively works with this condition, especially in SC systems. Here we will implement FD-DFE iteratively to allow the error propagation due to the feedback filter to be limited to only one block.

The implementation of FF and FB filters and data detection is iterated N_L times. At iteration L $(L = 1,2, \ldots . N_L)$, the vectors F_L & B_L containing both the FF and FB filter coefficients.

AS shown in Fig.3.2, the output of the equalizer can be expressed as

$$u_{k,i}^{L} = \frac{1}{N} \sum_{b=0}^{N-1} \left(F_{L,b} R_{k,b} + B_{L,b} \hat{S}_{L-1,b} \right) e^{j\frac{2\pi}{N} ib}, \tag{3.8}$$

where, $\hat{S}_{L-1,b} = \sum_{o=0}^{N-1} \hat{s}_{L-1,o}\, e^{-j\frac{2\pi}{N} 0b}$, b $= 0, . . \mathrm{N} - 1$.

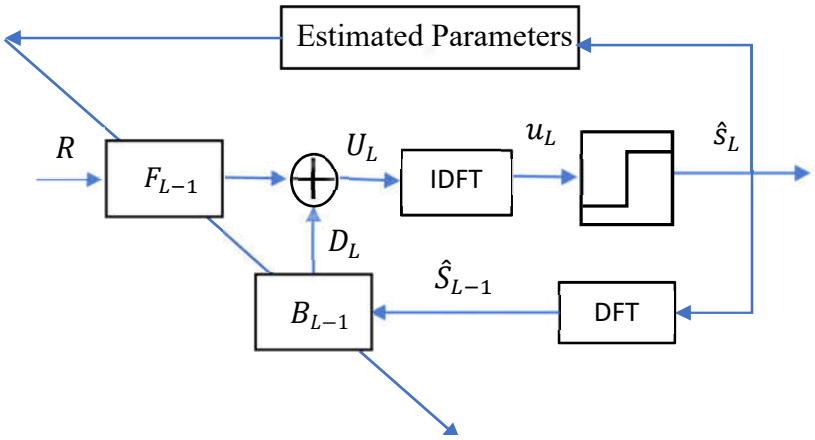

Figure 3.2: SC-FDMA iterative FD-E.

Assuming i.i.d sequences for the transmitted and detected data with zero mean, and statistically independent of noise, approach. the FF and FB filters are designed to minimize the MSE at the detection point similar to that of [86], that is

$$MSE = E\left(\left|u_{k,i}^{L} - s_{k,i}\right|^2\right), \tag{3.9}$$

$$MSE = \frac{1}{N^2}\sum_{b=0}^{N-1} E\left(\left|F_{L,b}R_{k,b} + B_{L,b}\hat{S}_{L-1,b} - S_{k,b}\right|^2\right), \tag{3.10}$$

$$MSE = \frac{1}{N^2}\sum_{b=0}^{N-1} E\left(\left|\left(F_{L,b}\bar{\bar{H}}_{k,b} - 1\right)S_{k,b} + F_{L,b}N_b + B_{L,b}\hat{S}_{L-1,b}\right|^2\right). \tag{3.11}$$

Using the same derivations and constraints as in [17] for SC-FDE, we can get the FF and FB filter coefficients for SC-FDMA, respectively as follows:

$$F_{L,b} = \frac{N\sigma_s^2\left(1 - \frac{\left|r_{s,\hat{s}_{L-1}}\right|^2}{\sigma_s^2\sigma_{\hat{s}_{L-1}}^2}\beta_{k,L}\right)\bar{\bar{H}}_{k,b}}{M\sigma_v^2 + N\sigma_s^2\left(1 - \frac{\left|r_{s,\hat{s}_{L-1}}\right|^2}{\sigma_s^2\sigma_{\hat{s}_{L-1}}^2}\left|\bar{\bar{H}}_{k,b}\right|^2\right)}, \tag{3.12}$$

$$B_{L,b} = -\frac{r_{s,\hat{s}_{L-1}}}{\sigma_{\hat{s}_{L-1}}^2}\left(F_{L,b}\bar{\bar{H}}_{k,b} - \beta_{k,L}\right), \tag{3.13}$$

where

$$\beta_{k,L} = \left(\frac{\sum_{b=0}^{N-1} \frac{\sigma_s^2 \left|\bar{\bar{H}}_{k,b}\right|^2}{M\sigma_v^2 + N\sigma_s^2 \left(1 - \frac{\left|r_{s,\hat{s}_{L-1}}\right|^2}{\sigma_s^2 \sigma_{\hat{s}_{L-1}}^2} \left|\bar{\bar{H}}_{k,b}\right|^2\right)}}{1 + \sum_{b=0}^{N-1} \frac{\frac{\left|r_{s,\hat{s}_{L-1}}\right|^2}{\sigma_s^2} \left|\bar{\bar{H}}_{k,b}\right|^2}{M\sigma_v^2 + N\sigma_s^2 (1 - \frac{\left|r_{s,\hat{s}_{L-1}}\right|^2}{\sigma_s^2 \sigma_{\hat{s}_{L-1}}^2} \left|\bar{\bar{H}}_{k,b}\right|^2)}} \right) \tag{3.14}$$

and the estimation of parameters $\sigma_{\hat{s}_{L-1}}^2$ and $r_{s,\hat{s}_{L-1}}$ are the same as [42]. for L=1, with no recognized data, we initiate

$$\hat{S}_{L-1,b} = 0 \ , \ b = 0,1, \dots \dots \dots M-1. \tag{3.15}$$

3.2.3. Phase Noise

PHN emerging from imperfections in the local-oscillator (LO) can be modelled as a non-stationary random process called Wiener process with variance rises linearly with time. This model generates from free-running oscillator [87]. The PHN power spectrum density (PSD) follows the Lorentzian-shape, which produces Inter-Carrier- Interference (ICI) between adjacent subcarriers [88].

The TD received signals corresponding to all N_u users for t^{th} SC-FDMA symbol in the presence of the transceiver PHN given by

$$r^t = \delta_r^t \sum_{l=0}^{N_u-1} H_l^t \, \delta_l^t g_l^t + n^t, \tag{3.16}$$

where H_l^{th} is the $(M \times M)$ channel circular convolution matrix with first column comprises the impulse response of the channel between the l^{th} user's MS and the BS, n^{th} is the

$(M \times 1)$ AWGN with variance σ_n^2, and δ_r^t and δ_l^t are the diagonal PHN matrices of both RX and TX, respectively, and are given by

$$\delta_r^t = diag(e^{\emptyset_0^{t,r}}, e^{\emptyset_1^{t,r}}, \dots\dots, e^{\emptyset_{M-1}^{t,r}}), \tag{3.17}$$

$$\delta_l^t = diag\left(e^{\emptyset_0^{t,l}}, e^{\emptyset_1^{t,l}}, \dots\dots, e^{\emptyset_{M-1}^{t,l}}\right), \tag{3.18}$$

where $\emptyset_b^{t,r}$ and $\emptyset_b^{t,l}$ are the samples of PHN affecting the t^{th} SC-FDMA TD symbol at b^{th} sample.

The 1^{st} order auto-regressive model [89] is employed to model the transceiver PHN as

$$\emptyset_b^{t,r} = \emptyset_{b-1}^{t,r} + \gamma_b^{t,r}, \tag{3.19}$$

$$\emptyset_b^{t,l} = \emptyset_{b-1}^{t,l} + \gamma_b^{t,l}, \tag{3.20}$$

where $\gamma_b^{t,r}$ and $\gamma_b^{t,l}$ are i.i.d Gaussian random variables, respectively, with variances $\sigma_r^2 = \frac{2\pi\alpha_r}{Nf_{sub}}$, $\sigma_l^2 = \frac{2\pi\alpha_l}{Nf_{sub}}$ and zero means. The model has zero initial values. The parameters α_l and α_r refer to the two-sided 3-dB linewidth of the Lorentzian-PSD of the LO at the BS and user's MS, respectively, and f_{sub} refers to the spacing of subcarriers in Hz.

The low pass nature of receiver PHN enables us to switch between the matrices of both channel and receiver PHN, and this simplifies the transceiver PHN model [90]-[91]. Therefore, the received signals can be written as

$$r^t = \sum_{L=0}^{N_u-1} H_L^t \, \delta_L^t \, g_L^t + n^t \,, \tag{3.21}$$

where $\delta_L^t = \delta_r^t \times \delta_l^t$ is the powerful transceiver PHN matrix given by

$$\delta_L^t = diag\left(e^{\emptyset_0^{t,L}}, e^{\emptyset_1^{t,L}}, \dots, \dots, e^{\emptyset_{M-1}^{t,L}}\right), \tag{3.22}$$

$$\emptyset_b^{t,L} = \emptyset_{b-1}^{t,L} + \gamma_b^{t,L}, \tag{3.23}$$

where $\gamma_b^{t,L} \sim \mathcal{N}(0, \sigma_L^2 = \frac{2\pi(\alpha_r+\alpha_l)}{Nf_{sub}})$ is i.i.d Gaussian random variable. Hence, the transceiver PHN is modelled as transmit-only PHN with effective 3-dB bandwidth of $\alpha_L = \alpha_r + \alpha_l$.

Without loss of generality, we will drop the SC-FDMA symbol index. After M-FFT transformation and demapping, the FD received signal for the k^{th} user will be given by

$$R_k = \bar{\widehat{H}}_k \bar{\hat{\delta}}_k F_N s_k + \quad T_k^H \sum_{L=0, L\neq k}^{N_u-1} F_M H_L \, \delta_L \, F_M^H T_L F_N s_L + T_k^H F_M \, n \, , \tag{3.24}$$

That is

$$R_k = desired\ signal + SUI + IUI + noise \, , \tag{3.25}$$

where $\bar{\widehat{H}}_k = T_k^H \widehat{H}_k T_k$, is a $(N \times N)$ diagonal sub-matrix of the FD transformation ($(M \times M)\, \widehat{H}_k$) of the circulant channel matrix H_k and $\bar{\hat{\delta}}_k$ is a $(N \times N)$ circulant sub-matrix of the FD transformation ($(M \times M)\, \hat{\delta}_k$) of the PHN diagonal δ_k matrix .

The self-user interference (USI) term results from the non-diagonal elements of the $\bar{\hat{\delta}}_k$ matrix, and the inter-user interference (IUI) term results from the other users.

3.3. Iterative Algorithm

The low-pass characteristics and slow variation of PHN give the possibility to estimate and compensate its effects iteratively. We will employ the iterative nature of the frequency domain equalization technique to also compensate for the PHN.

Next, we describe our proposed iterative FD-E and PHN compensation technique in detail as shown in Fig. 3.3.

1. Set the initial value of the detected date $\hat{S}_L = 0$ and initialize the iteration counter with L =1.
2. Estimate parameters $\sigma^2_{\hat{S}_{L-1}}$ and $r_{s,\hat{s}_{L-1}}$ as in [17].
3. Compute FF and FB filters coefficients from (3.12), (3.13) and (3.14).
4. Perform FD Equalization $U_L = F_L R_k + B_L \hat{S}_{L-1}$.
5. Perform PHN estimation and compensation in TD [92] using a window of maximum size 2c, and performing least-square estimation over this window, the PHN estimation can be given as

$$\hat{\vartheta}_i = \frac{\hat{s}_{\max(1,i-c):\min(N,i+c)} u_{\max(1,i-c):\min(N,i+c)}}{\left\|\hat{s}_{\max(1,i-c):\min(N,i+c)}\right\|_2^2} \quad \forall\, i = 1, \dots, N \tag{3.26}$$

Compensate the PHN by $diag\ (\hat{\vartheta})^{-1} u$.

6. Take the decisions of $diag\ (\hat{\vartheta})^{-1} u$ and construct the detected date $\hat{S}_L$.
7. Set L=L+1 and examine the stopping criteria if it ok, break the algorithm, otherwise move to step 2 and repeat the procedure.

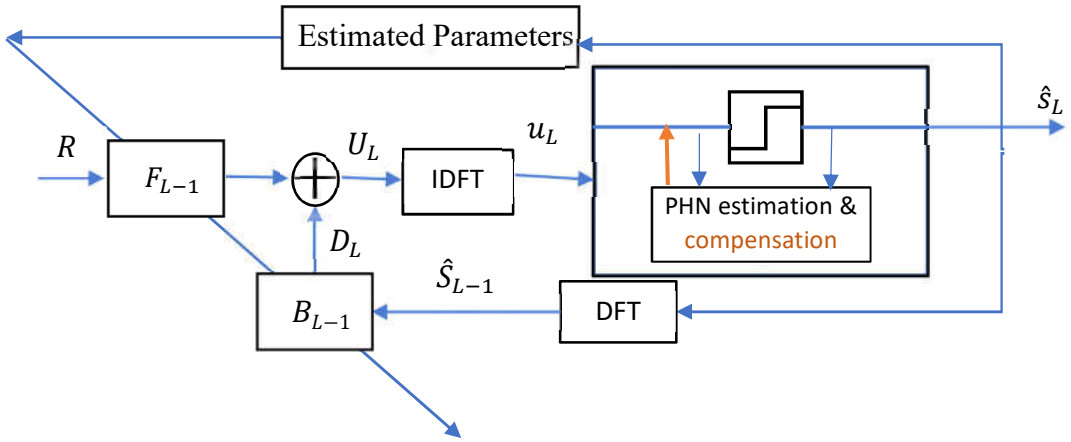

Figure 3.3: SC-FDMA PHN Compensation.

3.4. Simulation Results

In this section, the simulations are conducted to test the performance of our proposed I-FD-E & PHN compensation algorithm. The SC-FDMA system will be modelled by N =64, M=512($\text{sub} - \text{carriers} = 512$),subcarrier spacing $= 15$ KHz ,cyclic-prefix length=16, vehicular A channel model , QPSK modulation format , and the PHN parameters are set to $\alpha_r = 10$ and $\alpha_l = 65$ corresponding to the oscillator's PSD of$-58\frac{dBc}{Hz}$ and $-49.85\ \frac{dBc}{Hz}$ at 1 kHz frequency offset from f_c respectively.

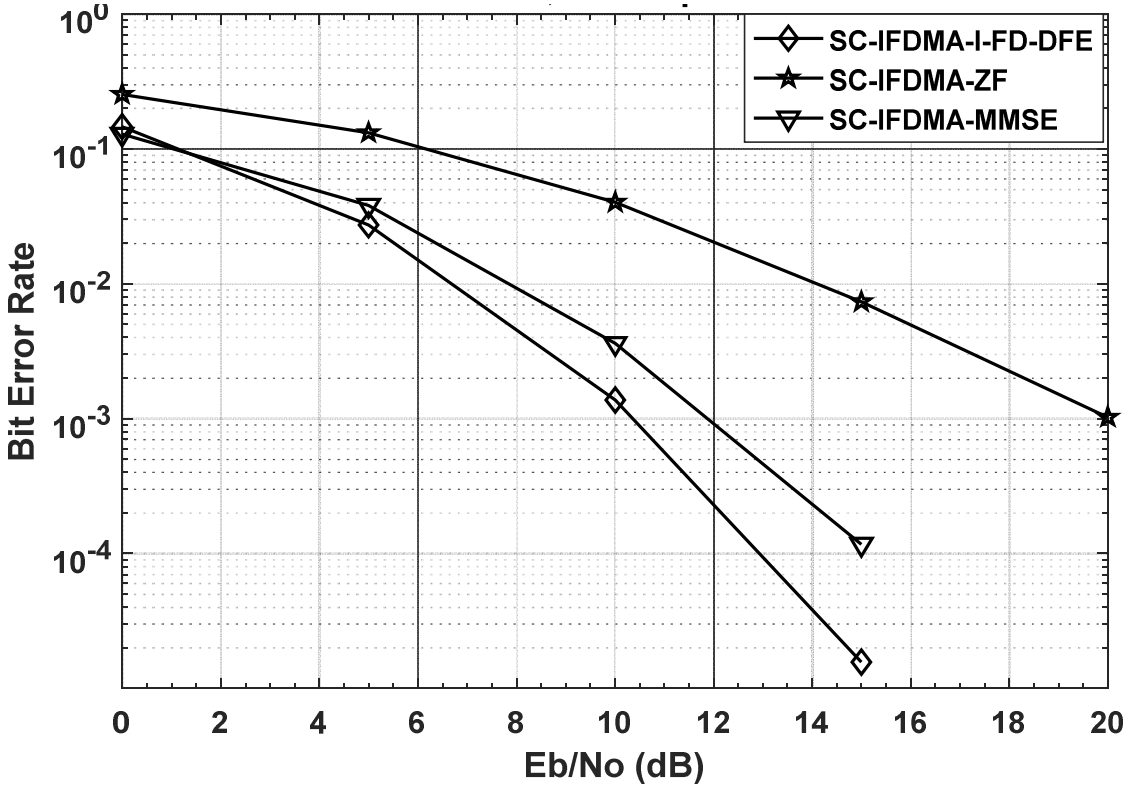

Figure 3.4: Comparison between various types of FD equalizers.

It is clear that the Bit Error Rate (BER) performance of the Iterative-FD-E in Fig.3.4 outperforms that of both linear equalizers ZF and MMSE in Vehicular A channel model. As can be depicted from this figure, a BER of 10^{-4} is achieved for an SNR of 13 dB compared to 15 dB for the MMSE. Again of $2dB$ in favor of our proposed scheme is achieved.

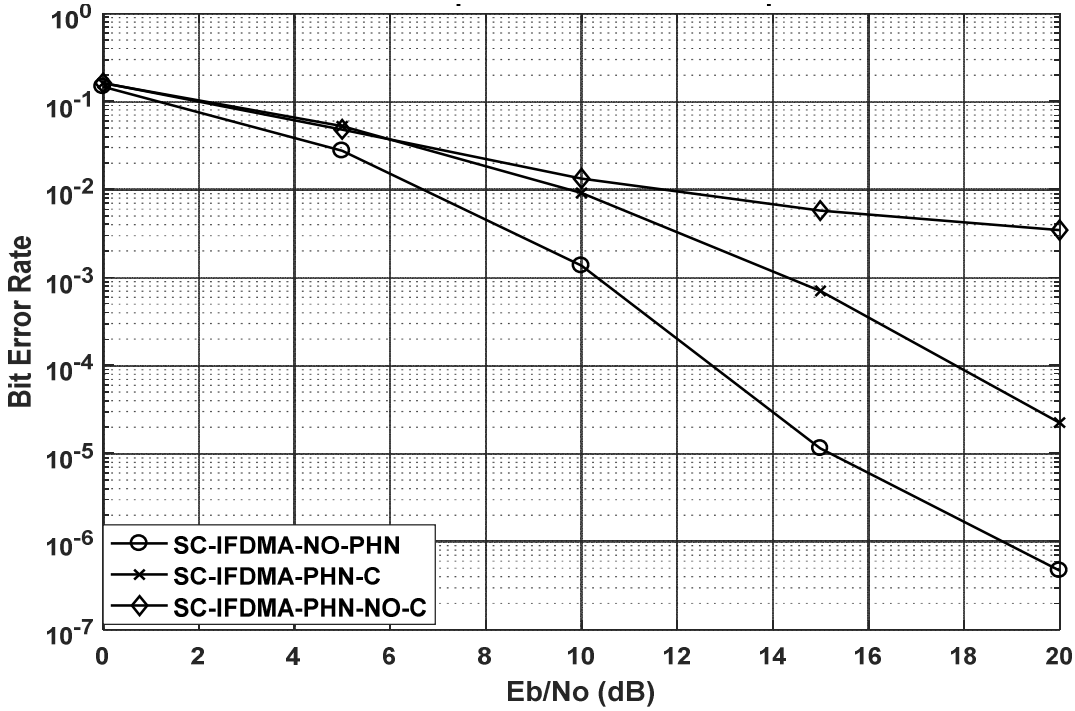

Figure 3.5: Iterative Equalization and PHN Compensation.

Also, from Fig. 3.5 and Fig. 3.6 we can note that Iterative-FD-E algorithm can be utilized to compensate PHN, so we can conclude that the our I-FD-E is robust to ICI. Fig. 3.6 shows the performance of the proposed algorithm against versus levels of PHN at SNR=20dB.

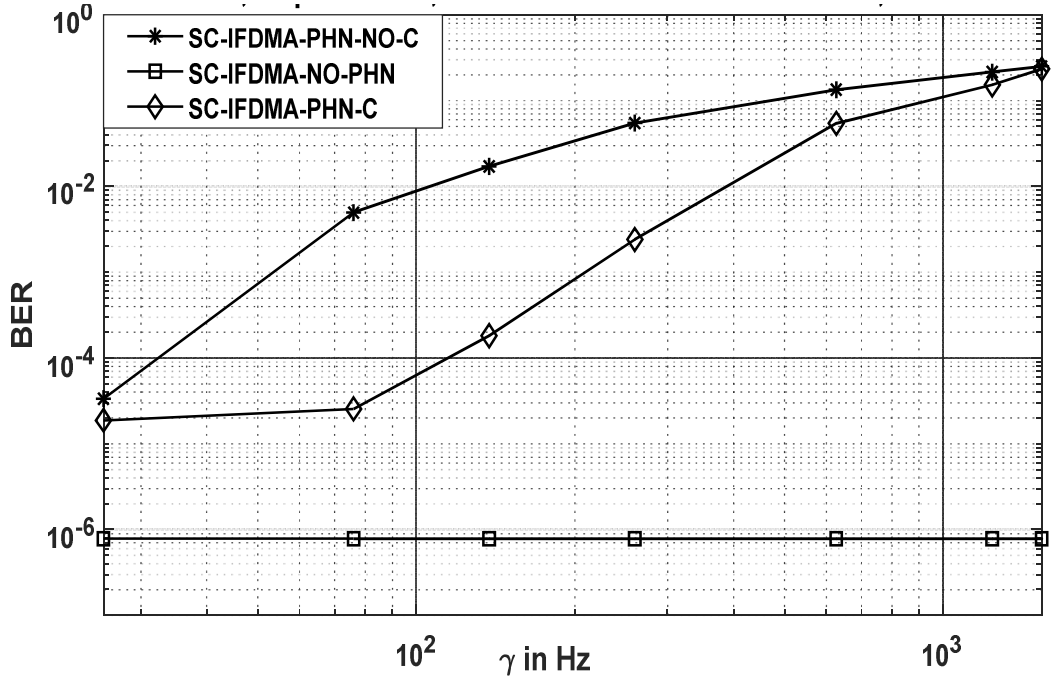

Figure 3.6: PHN compensation with and without reliability V.S PHN levels.

3.5. Conclusion

In this chapter, the iterative nature of the Iterative-FD-DFE in SC-FDMA to jointly eliminate ISI and compensate PHN simultaneously was utilized. Also, the simulation results support our findings which are robustness and notable performance gain under critical conditions of the channels and transceiver PHN Levels.

CHAPTER 4

ERROR PROPAGATION IMPROVEMENT

The incorrect feedback decisions will become more serious especially in the deep fading and make the error propagate through the equalization process. To alleviate its effects many algorithms have been proposed for this purpose [80][81][82]. In this work we propose a new technique to combat this effect. Excellent results are obtained. More details about these techniques are given next.

4.1.Feedback Reliability

The proposed technique to improve the FD-E process is based on the reliability of the detected symbols. After we get the reliability for each detected symbol, we pick and arrange the symbols with the greatest reliability value in descending order and index them. Then the symbols with the highest reliability will be chosen in the decision feedback.

The idea of reliability is not new, (see e.g.,[93]-[94]). Its working criteria only rely on the relative measure of the distance between the received constellation point and its neighbors to find the confidence levels.

To describe the adopted way, we examine as an interesting example. The constellation presented in Fig.4.1 from [93]. In this example, both equalized symbols $\hat{S}_1$ and $\hat{S}_2$ have the same distance to the nearest constellation point, S. Despite both symbols being equidistant from S, they have various reliability values. This is because the distances between these two points and their respective next-nearest neighbors are different. Clearly, note that S_a is the next nearest neighbour of $\hat{S}_1$ and S_b is the next nearest neighbour of $\hat{S}_2$. Also, given

that $\hat{S}_1$ and $\hat{S}_2$ are equidistant from, S, it is obvious that $\hat{S}_2$ is more reliable than $\hat{S}_1$ and in relevant terms we have

$$\frac{|\hat{s}_2 - s|}{|\hat{s}_2 - s_b|} < \frac{|\hat{s}_1 - s|}{|\hat{s}_1 - s_a|}. \tag{4.1}$$

This suggests the next reliability metric $R(n)$

$$R(n) = -\log\left(\frac{|\hat{s} - \lfloor\hat{s}\rceil|}{|\hat{s} - \lfloor\hat{s}\rceil_{NN}|}\right), \tag{4.2}$$

where $\lfloor\hat{S}\rceil$ denotes rounding to the nearest constellation point while $\lfloor\hat{S}\rceil_{NN}$ denotes rounding to the next nearest constellation point.

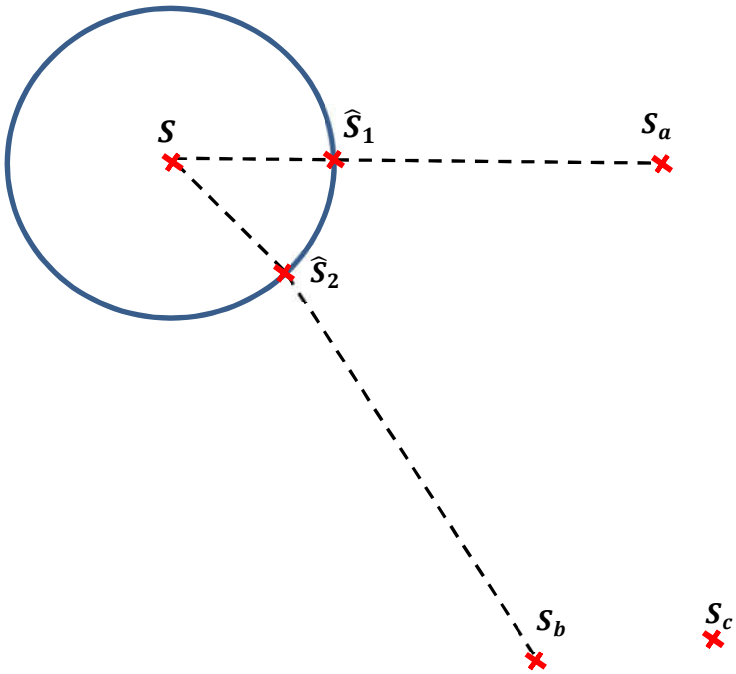

Figure 4.1: Geometrical representation of the adopted reliability criteria.

Consequently, after determining the reliability of all symbols, order the reliabilities in descending order $R(n_1) \geq R(n_2) \geq R(n_3) \geq \cdots \geq R(n_K)$ and take the modules of these quantities, $|R|$, with the greatest reliability.

Hence, after constructing the detected symbols $\hat{S}_L$ in step 6 (algorithm devised in chapter 3), we calculate the reliability and take the $|R|$ symbols with the greatest reliability in feedback, then go to step 7 (algorithm devised in chapter 3).

4.1.1. Simulation Results

The simulation to test reliability will be conducted here with the same parameters of SC-FDMA, PHN and channel environment given in chapter 3.

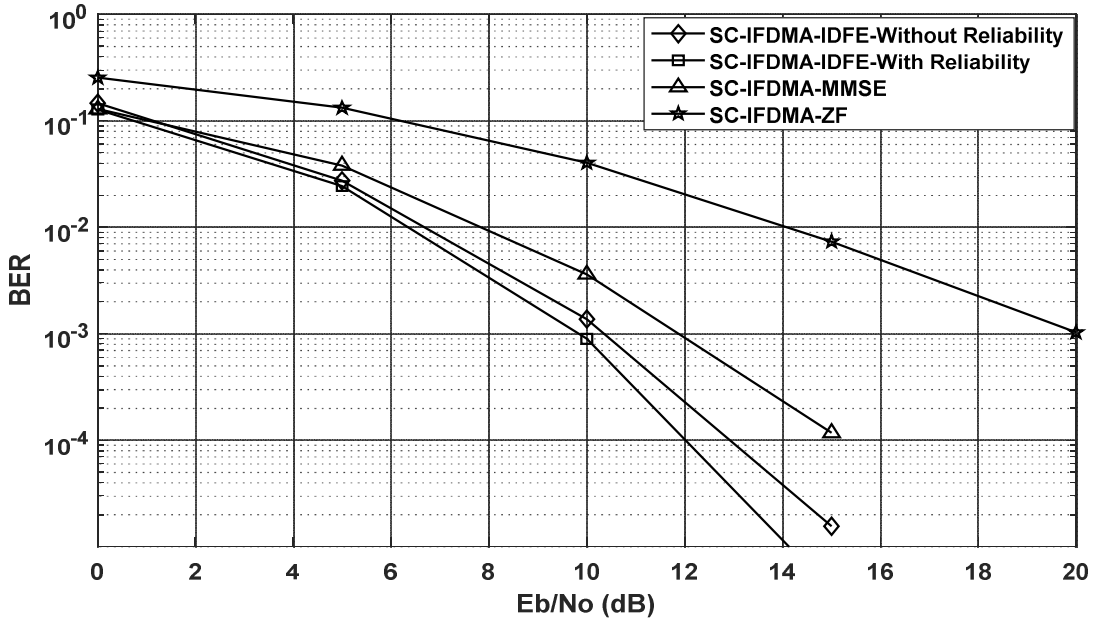

Figure 4.2: Comparison between various types of FD Equalizers.

It is clear that the Bit Error Rate (BER) performance of the Iterative-FD-E shown in Fig.4.2 in vehicular A channel model is improved by when using the reliability test. Here as can be seen from this figure, we can achieve BER=10^{-4} at 12 dB Compared to 13 dB in iterative FD-E without reliability and 15 dB in MMSE. A great improvement in performance is obtained through the use of this approach. Of course, there is a price to pay, which has to do with the computational complexity.

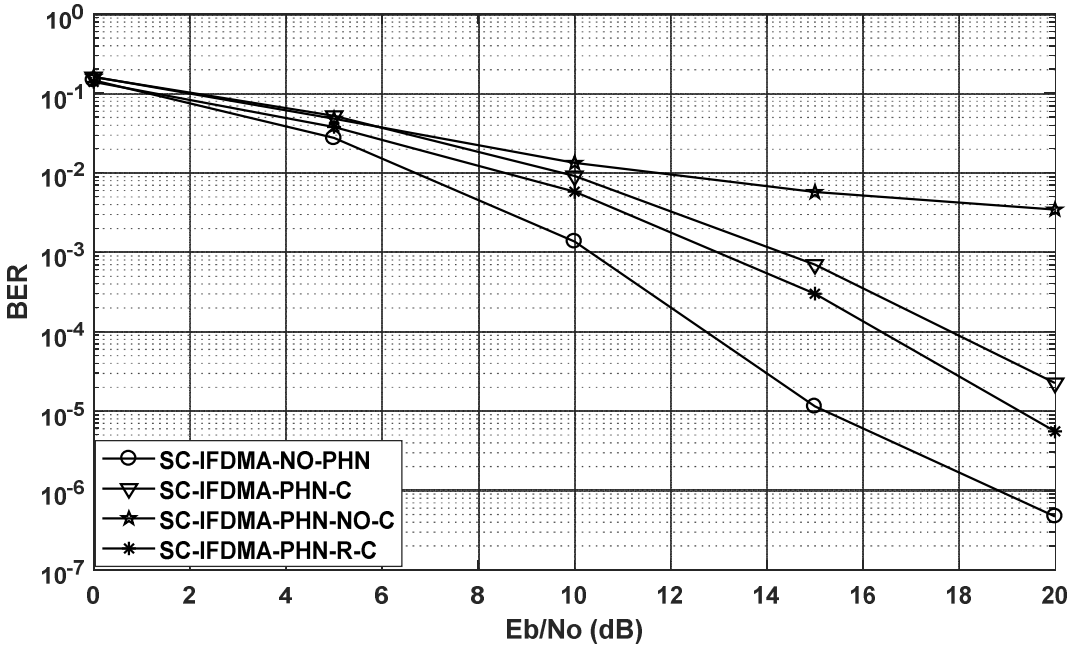

Figure 4.3: Iterative equalization and PHN compensation.

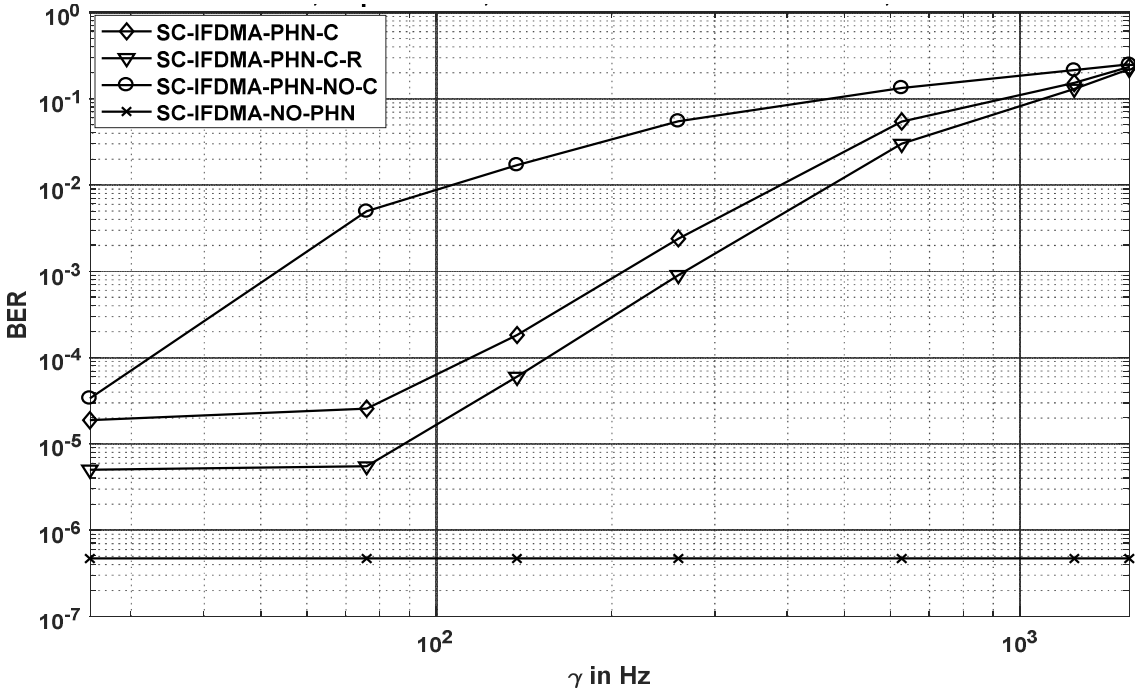

Figure 4.4: PHN compensation With & Without reliability V.S PHN levels.

Also, from Fig. 4.3 and Fig. 4.4 we can note that the iterative-FD-E algorithm in PHN Compensation will improve the performance by utilizing the proposed reliability.

4.2. Feedback Correlation Metric

Also, we can alleviate the effects of the incorrect feedback decisions by improving the calculation of the correlation metric $r_{s,\hat{s}}$ (between s and $\hat{s}$).

To calculate the feedback correlation metric, we assume the noise at the output of the I-FD-E is Gaussian distributed and utilizing QAM as a digital modulation technique. The i^{th} time domain detected symbol at the L^{th} iteration can be written mathematically as

$$\hat{s}_i = s_i + e_i. \tag{4.3}$$

Therefore, $r_{s,\hat{s}}$ can be given as

$$\begin{aligned} r_{s,\hat{s}} &= E[s_i \hat{s}_i{}^*], \\ &= E[s_i (s_i + e_i)^*], \\ &= 1 + E[s_i e^*{}_i]. \end{aligned} \tag{4.4}$$

Let $(.)_{R,i}$ and $(.)_{I,i}$ denote the in phase and quadrature components, respectively. Since $s_{R,i}(s_{I,i})$ and $e^*{}_{I,i}\,(e^*{}_{R,i})$ are independent, therefore, $E[s_i e^*{}_i] = E\left[s_{R,i} e^*{}_{R,i}\right] + E\left[s_{I,i} e^*{}_{I,i}\right]$. In case of a rectangular QAM constellation $E\left[s_{R,i} e^*{}_{R,i}\right] = E\left[s_{I,i} e^*{}_{I,i}\right]$ and, therefore, $E[s_i e^*{}_i] = 2\,E\left[s_{R,i} e^*{}_{R,i}\right]$. Each single point in $P-$QAM constellation can be considered as a combination of two orthogonal signals from $\sqrt{P}-$PAM constellation. Hence, the expectation $E\left[s_{R,i} e^*{}_{R,i}\right]$ is the same as for a PAM signal and is given by

$$E\left[s_{R,i} e^*{}_{R,i}\right] = \sum_{k=1}^{P} \sum_{j=1}^{P} s^k{}_{R,i}\, e^{j*}{}_{R,i}\, p\left(s^k{}_{R,i}, e^{j*}{}_{R,i}\right). \tag{4.5}$$

Using the total probability theorem, we get

$$\begin{aligned} p\left(s^k{}_{R,i}, e^{j*}{}_{R,i}\right) &= p\left(s^k{}_{R,i}/e^{j*}{}_{R,i}\right) p\left(e^{j*}{}_{R,i}\right) \\ &= p\left(e^{j*}{}_{R,i}/s^k{}_{R,i}\right) p\left(s^k{}_{R,i}\right) \end{aligned} \tag{4.6}$$

$p\left(e^{j*}{}_{R,i}/s^k{}_{R,i}\right) = 0$, when $j = k$, there is no error

Since all symbols of the constellation are equal probable, therefore, the expectation is given as

$$E\left[s_{R,i}e^{*}{}_{R,i}\right]=\frac{1}{P}\sum_{k=1}^{P}s^{k}{}_{R,i}\sum_{j=1,j\neq k}^{P}e^{j*}{}_{R,i}p\left(e^{j*}{}_{R,i}/s^{k}{}_{R,i}\right). \tag{4.7}$$

Next, the expectation is derived for a 64-QAM (for $P = 2, 4$ *and* 16) where the same steps should be followed. The 8-PAM constellation for this purpose is shown in Fig. 26 where the constellation points are located at $\{\pm1, \pm3, \ldots\ldots\ldots\ldots, \pm(\sqrt{P}-1)\}$, then normalized with average energy to end with unit average energy.

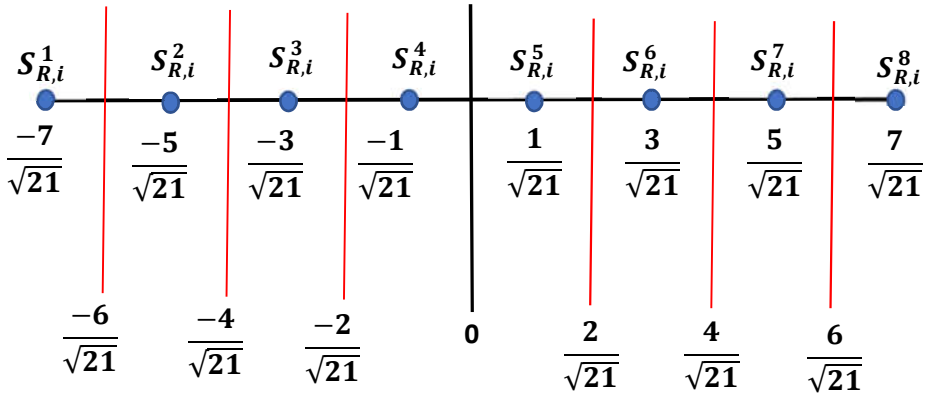

Figure 4.5: Normalized 8-PAM constellation.

Next, the term $s^{k}{}_{R,i}\sum_{j=1,j\neq k}^{P}e^{j*}{}_{R,i}p\left(e^{j*}{}_{R,i}/s^{k}{}_{R,i}\right)$ in (4.7) is evaluated for $k = 1$, and can be shown to be

$$\begin{aligned}
&s^{1}{}_{R,i}\sum_{j=2}^{8}e^{j*}{}_{R,i}p\left(e^{j*}{}_{R,i}/s^{1}{}_{R,i}\right)\\
&\quad=\frac{-7}{\sqrt{21}}\left[\frac{2}{\sqrt{21}}p\left(\frac{-4}{\sqrt{21}}>\hat{s}^{1}{}_{R,i}>\frac{-6}{\sqrt{21}}\right)\right.\\
&\quad+\frac{4}{\sqrt{21}}p\left(\frac{-2}{\sqrt{21}}>\hat{s}^{1}{}_{R,i}>\frac{-4}{\sqrt{21}}\right)+\frac{6}{\sqrt{21}}p\left(0>\hat{s}^{1}{}_{R,i}>\frac{-2}{\sqrt{21}}\right)\\
&\quad+\frac{8}{\sqrt{21}}p\left(\frac{2}{\sqrt{21}}>\hat{s}^{1}{}_{R,i}>0\right)+\frac{10}{\sqrt{21}}p\left(\frac{4}{\sqrt{21}}>\hat{s}^{1}{}_{R,i}>\frac{2}{\sqrt{21}}\right)\\
&\quad\left.+\frac{12}{\sqrt{21}}p\left(\frac{6}{\sqrt{21}}>\hat{s}^{1}{}_{R,i}>\frac{4}{\sqrt{21}}\right)+\frac{14}{\sqrt{21}}p\left(\hat{s}^{1}{}_{R,i}>\frac{6}{\sqrt{21}}\right)\right].
\end{aligned} \tag{4.8}$$

We have $\hat{s}^1{}_{R,i} = s^1{}_{R,i} + e$ .Also, we have $s^1{}_{R,i} = \frac{-7}{\sqrt{21}}$ and $e \sim N(0, \sigma^2)$ so we will make random variable transformation to get

$$
\begin{aligned}
& s^1{}_{R,i} \sum_{j=2}^{8} e^{j*}{}_{R,i} p\left(e^{j*}{}_{R,i} / s^1{}_{R,i}\right) \\
&= \frac{-7}{21}\Big[2\, p\left(\frac{3}{\sqrt{21}} > e > \frac{1}{\sqrt{21}}\right) + 4\, p\left(\frac{5}{\sqrt{21}} > e > \frac{3}{\sqrt{21}}\right) \\
&+ 6\, p\left(\frac{7}{\sqrt{21}} > e > \frac{5}{\sqrt{21}}\right) + 8\, p\left(\frac{9}{\sqrt{21}} > e > \frac{7}{\sqrt{21}}\right) \\
&+ 10\, p\left(\frac{11}{\sqrt{21}} > e > \frac{9}{\sqrt{21}}\right) + 12\, p\left(\frac{13}{\sqrt{21}} > e > \frac{11}{\sqrt{21}}\right) \\
&+ 14\, p\left(e > \frac{13}{\sqrt{21}}\right)\Big].
\end{aligned}
\tag{4.9}
$$

Since,

$$
p\left(\tfrac{1}{\sqrt{21}} < e < \tfrac{3}{\sqrt{21}}\right) = p\left(e > \tfrac{1}{\sqrt{21}}\right) - p\left(e > \tfrac{3}{\sqrt{21}}\right). \tag{4.10}
$$

A graphical explanation of (4.10) is shown in Fig.4.6

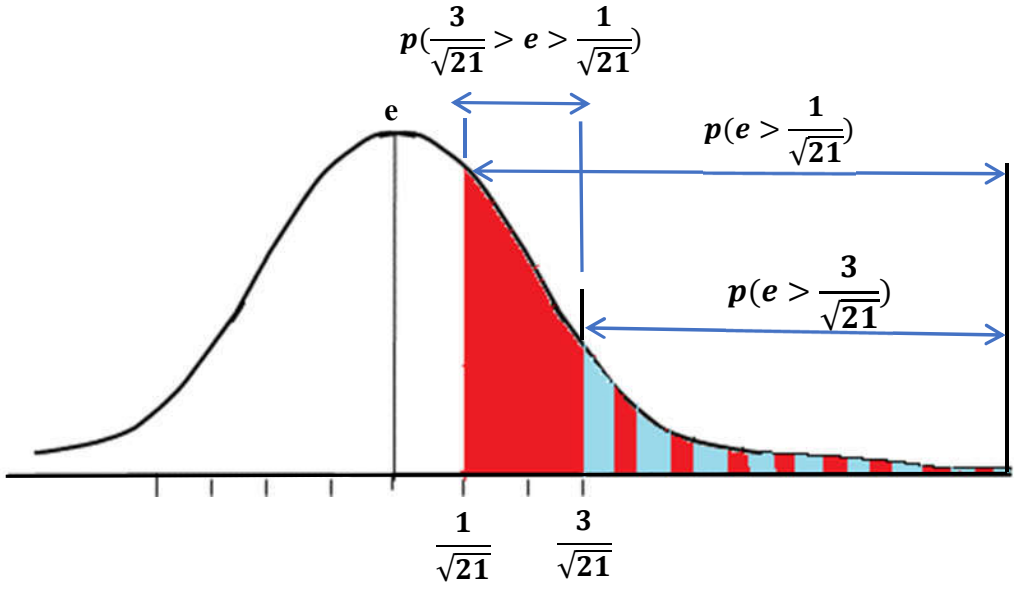

Figure 4.6: Normal Distribution.

The derived expectation will be

$$s^1{}_{R,i}\sum_{j=2}^{8} e^{j*}{}_{R,i}p\left(e^{j*}{}_{R,i}/s^1{}_{R,i}\right) = \frac{-7}{21}\left[2\,p\left(e > \frac{1}{\sqrt{21}}\right) - 2\,p\left(e > \frac{3}{\sqrt{21}}\right) + 4\,p\left(e > \frac{3}{\sqrt{21}}\right) - 4\,p\left(e > \frac{5}{\sqrt{21}}\right) + 6\,p\left(e > \frac{5}{\sqrt{21}}\right) - 6\,p\left(e > \frac{7}{\sqrt{21}}\right) + 8\,p\left(e > \frac{7}{\sqrt{21}}\right) - 8\,p\left(e > \frac{9}{\sqrt{21}}\right) + 10\,p\left(e > \frac{9}{\sqrt{21}}\right) - 10\,p\left(e > \frac{11}{\sqrt{21}}\right) + 12\,p\left(e > \frac{11}{\sqrt{21}}\right) - 12\,p\left(e > \frac{13}{\sqrt{21}}\right) + 14\,p\left(e > \frac{13}{\sqrt{21}}\right)\right], \tag{4.11}$$

which can be setup into the following:

$$s^1{}_{R,i}\sum_{j=2}^{8} e^{j*}{}_{R,i}p\left(e^{j*}{}_{R,i}/s^1{}_{R,i}\right) = \frac{-7}{21}\left[2\,p\left(e > \frac{1}{\sqrt{21}}\right) + 2\,p\left(e > \frac{3}{\sqrt{21}}\right) + 2\,p\left(e > \frac{5}{\sqrt{21}}\right) + 2\,p\left(e > \frac{7}{\sqrt{21}}\right) + 2\,p\left(e > \frac{9}{\sqrt{21}}\right) + 2\,p\left(e > \frac{11}{\sqrt{21}}\right) + 2\,p\left(e > \frac{13}{\sqrt{21}}\right)\right]. \tag{4.12}$$

Since,$Q(u) = \frac{1}{2\pi}\int_u^\infty \exp\left(-\frac{t^2}{2}\right)\,du = p(U > u)$. Figure 4.7 gives an explanation of the Q () function.

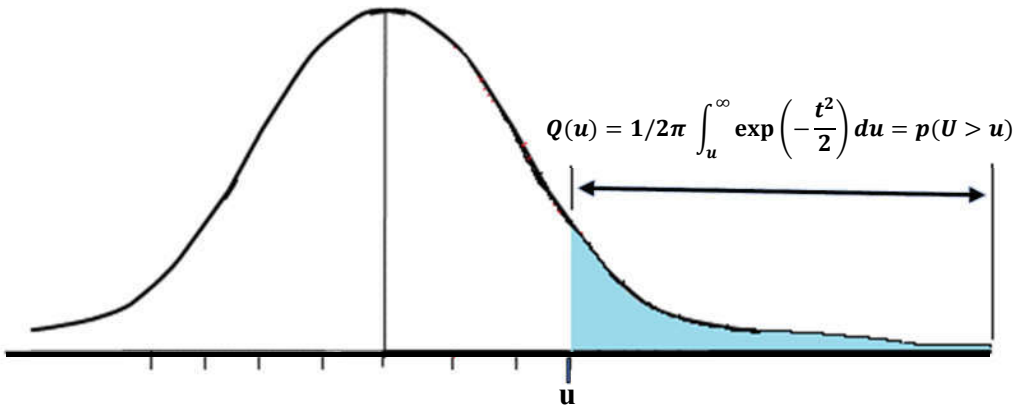

Figure 4.7: Q function .

Hence, (4.12) can be setup using the definition of the Q () function as follow:

$$
\begin{aligned}
&{s^1}_{R,i}\sum_{j=2}^{8} {e^{j*}}_{R,i}p\left({e^{j*}}_{R,i}/{s^1}_{R,i}\right) \\
&\qquad = \frac{-14}{21}\left[Q\left(\sqrt{\frac{1}{21\,\sigma^2}}\right) + Q\left(\sqrt{\frac{9}{21\,\sigma^2}}\right) + Q\left(\sqrt{\frac{25}{21\,\sigma^2}}\right)\right. \\
&\qquad + Q\left(\sqrt{\frac{49}{21\,\sigma^2}}\right) + Q\left(\sqrt{\frac{81}{21\,\sigma^2}}\right) + Q\left(\sqrt{\frac{121}{21\,\sigma^2}}\right) \\
&\qquad \left. + Q\left(\sqrt{\frac{169}{21\,\sigma^2}}\right)\right].
\end{aligned}
\tag{4.13}
$$

By considering the error variance $\sigma^2 = N_o = \frac{1}{N}\sum_{i=1}^{N}|\hat{s}_i - s_i|^2$, and $\gamma_{sPAM} = \frac{E_s}{2N_o}$ where $E_s = 1$, then (4.13) results in

$$
\begin{aligned}
&{s^1}_{R,i}\sum_{j=2}^{8} {e^{j*}}_{R,i}p\left({e^{j*}}_{R,i}/{s^1}_{R,i}\right) \\
&\qquad = \frac{-14}{21}\left[Q\left(\sqrt{\frac{1}{21\,N_o}}\right) + Q\left(\sqrt{\frac{9}{21\,N_o}}\right) + Q\left(\sqrt{\frac{25}{21\,N_o}}\right)\right. \\
&\qquad + Q\left(\sqrt{\frac{49}{21\,N_o}}\right) + Q\left(\sqrt{\frac{81}{21\,N_o}}\right) \\
&\qquad \left. + Q\left(\sqrt{\frac{121}{21\,N_o}}\right) Q\left(\sqrt{\frac{169}{21\,N_o}}\right)\right].
\end{aligned}
\tag{4.14}
$$

Substituting for $\gamma_{sPAM} = \frac{E_s}{2N_o}$ in (4.14) we get

$$
\begin{aligned}
&{s^1}_{R,i}\sum_{j=2}^{8}{e^{j*}}_{R,i}p\left({e^{j*}}_{R,i}/{s^1}_{R,i}\right)\\
&\quad=\frac{-14}{21}\left[Q\left(\sqrt{\frac{2\gamma_{sPAM}}{21}}\right)+Q\left(\sqrt{\frac{6\gamma_{sPAM}}{7}}\right)+Q\left(\sqrt{\frac{50\gamma_{sPAM}}{21}}\right)\right.\\
&\quad+Q\left(\sqrt{\frac{14\gamma_{sPAM}}{3}}\right)+Q\left(\sqrt{\frac{54\gamma_{sPAM}}{7}}\right)+Q\left(\sqrt{\frac{242\gamma_{sPAM}}{21}}\right)\\
&\quad\left.+Q\left(\sqrt{\frac{338\gamma_{sPAM}}{21}}\right)\right].
\end{aligned}
\tag{4.15}
$$

This expression is identical to the one for $k = 8$, and $Q(u)$ is approximated as [95]

$$
Q(u)\cong\frac{(1-\exp(-1.4u))\exp\left(-\frac{u^2}{2}\right)}{1.135\sqrt{2\pi u}}.
\tag{4.16}
$$

For the case when k=2, the following procedure is followed:

$$
\begin{aligned}
&{s^2}_{R,i}\sum_{j=1,j\neq 2}^{8}{e^{j*}}_{R,i}p\left({e^{j*}}_{R,i}/{s^2}_{R,i}\right)\\
&\quad=\frac{-5}{\sqrt{21}}\left[\frac{2}{\sqrt{21}}p\left(\frac{-2}{\sqrt{21}}>{\hat{s}^2}_{R,i}>\frac{-4}{\sqrt{21}}\right)\right.\\
&\quad+\frac{4}{\sqrt{21}}p\left(0>{\hat{s}^2}_{R,i}>\frac{-2}{\sqrt{21}}\right)+\frac{6}{\sqrt{21}}p\left(\frac{2}{\sqrt{21}}>{\hat{s}^2}_{R,i}>0\right)\\
&\quad+\frac{8}{\sqrt{21}}p\left(\frac{4}{\sqrt{21}}>{\hat{s}^2}_{R,i}>\frac{2}{\sqrt{21}}\right)+\frac{10}{\sqrt{21}}p\left(\frac{6}{\sqrt{21}}>{\hat{s}^2}_{R,i}>\frac{4}{\sqrt{21}}\right)\\
&\quad\left.+\frac{12}{\sqrt{21}}p\left({\hat{s}^2}_{R,i}>\frac{6}{\sqrt{21}}\right)-\frac{2}{\sqrt{21}}p\left({\hat{s}^2}_{R,i}<\frac{-6}{\sqrt{21}}\right)\right].
\end{aligned}
\tag{4.17}
$$

By using the same previous derivations, we end with

$$
\begin{aligned}
{s^2}_{R,i} \sum_{j=1, j\neq 2}^{8} {e^{j*}}_{R,i} p\left({e^{j*}}_{R,i} / {s^2}_{R,i}\right) \\
&= \frac{-10}{21}\left[Q\left(\sqrt{\frac{6\,\gamma_{sPAM}}{7}}\right) + Q\left(\sqrt{\frac{50\,\gamma_{sPAM}}{21}}\right) \right. \\
&\left. + Q\left(\sqrt{\frac{14\,\gamma_{sPAM}}{3}}\right) + Q\left(\sqrt{\frac{54\,\gamma_{sPAM}}{7}}\right) + Q\left(\sqrt{\frac{242\,\gamma_{sPAM}}{21}}\right)\right].
\end{aligned} \tag{4.18}
$$

Also, here this expression is identical to the one for $k = 7$.

For k =3, the following is done

$$
\begin{aligned}
{s^3}_{R,i} \sum_{j=1, j\neq 3}^{8} {e^{j*}}_{R,i} p\left({e^{j*}}_{R,i} / {s^3}_{R,i}\right) \\
&= \frac{-3}{\sqrt{21}}\left[\frac{2}{\sqrt{21}} p\left(\frac{-2}{\sqrt{21}} > {\hat{s}^3}_{R,i} > 0\right) + \frac{4}{\sqrt{21}} p\left(0 > {\hat{s}^3}_{R,i} > \frac{2}{\sqrt{21}}\right)\right. \\
&+ \frac{6}{\sqrt{21}} p\left(\frac{2}{\sqrt{21}} > {\hat{s}^3}_{R,i} > \frac{4}{\sqrt{21}}\right) + \frac{8}{\sqrt{21}} p\left(\frac{4}{\sqrt{21}} > {\hat{s}^3}_{R,i} > \frac{8}{\sqrt{21}}\right) \\
&+ \frac{10}{\sqrt{21}} p\left({\hat{s}^3}_{R,i} > \frac{6}{\sqrt{21}}\right) - \frac{2}{\sqrt{21}} p\left(\frac{-4}{\sqrt{21}} > {\hat{s}^3}_{R,i} > \frac{-6}{\sqrt{21}}\right) \\
&\left. - \frac{4}{\sqrt{21}} p\left({\hat{s}^3}_{R,i} < \frac{-6}{\sqrt{21}}\right)\right].
\end{aligned} \tag{4.19}
$$

We have ${\hat{s}^3}_{R,i} = {s^3}_{R,i} + e$, also, we have ${s^3}_{R,i} = \frac{-3}{\sqrt{21}}$ and $e \sim N(0, \sigma^2)$ so we will make random variable transformation to get

$$
\begin{aligned}
{s^3}_{R,i} \sum_{j=1, j\neq 3}^{8} {e^{j*}}_{R,i} p\left({e^{j*}}_{R,i} / {s^3}_{R,i}\right) \\
&= \frac{-3}{21}\left[2\, p\left(\frac{1}{\sqrt{21}} > e > \frac{3}{\sqrt{21}}\right) + 4\, p\left(\frac{3}{\sqrt{21}} > e > \frac{5}{\sqrt{21}}\right)\right. \\
&+ 6\, p\left(\frac{5}{\sqrt{21}} > e > \frac{7}{\sqrt{21}}\right) + 8\, p\left(\frac{7}{\sqrt{21}} > e > \frac{9}{\sqrt{21}}\right) \\
&\left. + 10\, p\left(e > \frac{9}{\sqrt{21}}\right) - 2\, p\left(\frac{-1}{\sqrt{21}} > e > \frac{-3}{\sqrt{21}}\right) - 4\, p\left(e < \frac{-3}{\sqrt{21}}\right)\right]
\end{aligned}
$$

$$= \frac{-3}{21}\Big[2\,p\left(e > \frac{1}{\sqrt{21}}\right) - 2\,p\left(e > \frac{3}{\sqrt{21}}\right) + 4\,p\left(e > \frac{3}{\sqrt{21}}\right) - 4\,p\left(e > \frac{5}{\sqrt{21}}\right)$$
$$+ 6\,p\left(e > \frac{5}{\sqrt{21}}\right) - 6\,p\left(e > \frac{7}{\sqrt{21}}\right) + 8\,p\left(e > \frac{7}{\sqrt{21}}\right)$$
$$- 8\,p\left(e > \frac{9}{\sqrt{21}}\right) + 10\,p\left(e > \frac{9}{\sqrt{21}}\right) - 2\,p\left(e > \frac{-3}{\sqrt{21}}\right)$$
$$+ 2\,p\left(e > \frac{-1}{\sqrt{21}}\right) - 4\,p\left(e < \frac{-3}{\sqrt{21}}\right)\Big]$$

$$= \frac{-3}{21}\Big[2\,p\left(e > \frac{1}{\sqrt{21}}\right) + 2\,p\left(e > \frac{3}{\sqrt{21}}\right) + 2\,p\left(e > \frac{5}{\sqrt{21}}\right) + 2\,p\left(e > \frac{7}{\sqrt{21}}\right)$$
$$+ 2\,p\left(e > \frac{9}{\sqrt{21}}\right) - 2\,p\left(e > \frac{-3}{\sqrt{21}}\right) + 2\,p\left(e > \frac{-1}{\sqrt{21}}\right)$$
$$- 4\,p\left(e < \frac{-3}{\sqrt{21}}\right)\Big]$$

$$= \frac{-3}{21}\Big[2\,Q\left(\frac{1}{\sqrt{\sigma^2 21}}\right) + 2\,Q\left(\frac{3}{\sqrt{\sigma^2 21}}\right) + 2\,Q\left(\frac{5}{\sqrt{\sigma^2 21}}\right) + 2\,Q\left(\frac{7}{\sqrt{\sigma^2 21}}\right)$$
$$+ 2\,Q\left(\frac{9}{\sqrt{\sigma^2 21}}\right) - 2\,Q\left(\frac{-3}{\sqrt{\sigma^2 21}}\right) + 2\,Q\left(\frac{-1}{\sqrt{\sigma^2 21}}\right)$$
$$- 4\,Q\left(\frac{3}{\sqrt{\sigma^2 21}}\right)\Big]$$

$$= \frac{-6}{21}\Big[\,Q\left(\frac{1}{\sqrt{\sigma^2 21}}\right) + Q\left(\frac{3}{\sqrt{\sigma^2 21}}\right) + Q\left(\frac{5}{\sqrt{\sigma^2 21}}\right)$$
$$+ Q\left(\frac{7}{\sqrt{\sigma^2 21}}\right) \qquad + Q\left(\frac{9}{\sqrt{\sigma^2 21}}\right) - Q\left(\frac{-3}{\sqrt{\sigma^2 21}}\right)$$
$$+ Q\left(\frac{-1}{\sqrt{\sigma^2 21}}\right) - 2\,Q\left(\frac{3}{\sqrt{\sigma^2 21}}\right)\Big]$$

$$= \frac{-6}{21}\Big[\,Q\left(\frac{1}{\sqrt{\sigma^2 21}}\right) + Q\left(\frac{3}{\sqrt{\sigma^2 21}}\right) + Q\left(\frac{5}{\sqrt{\sigma^2 21}}\right) + Q\left(\frac{7}{\sqrt{\sigma^2 21}}\right)$$
$$+ Q\left(\frac{9}{\sqrt{\sigma^2 21}}\right) \quad - 1 \qquad + Q\left(\frac{3}{\sqrt{\sigma^2 21}}\right) + 1 - Q\left(\frac{1}{\sqrt{\sigma^2 21}}\right)$$
$$- 2\,Q\left(\frac{3}{\sqrt{\sigma^2 21}}\right)\Big]$$

$$= \frac{-6}{21}\Big[\,Q\left(\frac{5}{\sqrt{\sigma^2 21}}\right) + Q\left(\frac{7}{\sqrt{\sigma^2 21}}\right) + Q\left(\frac{9}{\sqrt{\sigma^2 21}}\right)\,\Big]$$

$$= \frac{-6}{21}\left[\,Q\left(\sqrt{\frac{50\ \gamma_{sPAM}}{21}}\right) + Q\left(\sqrt{\frac{14\ \gamma_{sPAM}}{3}}\right) + Q\left(\sqrt{\frac{54\ \gamma_{sPAM}}{7}}\right)\,\right]. \tag{4.20}$$

This expression is identical for $k = 6$.

For k=4,

$$
\begin{aligned}
{s^4}_{R,i} \sum_{j=1, j\neq 4}^{8} {e^{j*}}_{R,i} p\left({e^{j*}}_{R,i} / {s^4}_{R,i}\right) \\
&= \frac{-1}{\sqrt{21}}\left[\frac{2}{\sqrt{21}} p\left(\frac{2}{\sqrt{21}} > {\hat{s}^4}_{R,i} > 0\right)\right. \\
&+ \frac{4}{\sqrt{21}} p\left(\frac{4}{\sqrt{21}} > {\hat{s}^4}_{R,i} > \frac{2}{\sqrt{21}}\right) + \frac{6}{\sqrt{21}} p\left(\frac{6}{\sqrt{21}} > {\hat{s}^4}_{R,i} > \frac{4}{\sqrt{21}}\right) \\
&+ \frac{8}{\sqrt{21}} p\left({\hat{s}^4}_{R,i} > \frac{6}{\sqrt{21}}\right) - \frac{2}{\sqrt{21}} p\left(\frac{-2}{\sqrt{21}} > {\hat{s}^4}_{R,i} > \frac{-4}{\sqrt{21}}\right) \\
&\left. - \frac{4}{\sqrt{21}} p\left(\frac{-4}{\sqrt{21}} > {\hat{s}^4}_{R,i} > \frac{-6}{\sqrt{21}}\right) - \frac{6}{\sqrt{21}} p\left({\hat{s}^4}_{R,i} < \frac{-6}{\sqrt{21}}\right)\right].
\end{aligned}
\tag{4.21}
$$

By using the same previous derivations, we ended by

$$
{s^4}_{R,i} \sum_{j=1, j\neq 4}^{P} {e^{j*}}_{R,i} p\left({e^{j*}}_{R,i} / {s^4}_{R,i}\right) = -\frac{10}{21}\left[Q\left(\sqrt{\frac{14\ \gamma_{sPAM}}{3}}\right)\right]. \tag{4.22}
$$

This expression is same as for $k = 5$.

Now the expectation is given by summing (4.15), (4.18), (4.20) and (4.22) to get

$$
\begin{aligned}
E\left[s_{R,i} {e^*}_{R,i}\right] = \frac{-1}{84}\Bigg[&14\ Q\left(\sqrt{\frac{2\ \gamma_{sPAM}}{21}}\right) + 30\ Q\left(\sqrt{\frac{50\ \gamma_{sPAM}}{21}}\right) \\
&+ 40\ Q\left(\sqrt{\frac{14\ \gamma_{sPAM}}{3}}\right) + 30\ Q\left(\sqrt{\frac{54\ \gamma_{sPAM}}{7}}\right) \\
&+ 24\ Q\left(\sqrt{\frac{242\ \gamma_{sPAM}}{21}}\right) + 24\ Q\left(\sqrt{\frac{6\ \gamma_{sPAM}}{7}}\right) \\
&+ 14\ Q\left(\sqrt{\frac{338\ \gamma_{sPAM}}{21}}\right)\Bigg].
\end{aligned}
\tag{4.23}
$$

Now doing similar calculations for $P-QAM = 4$, we get $\sqrt{P}-PAM = 2$ which is shown in Fig.4.8

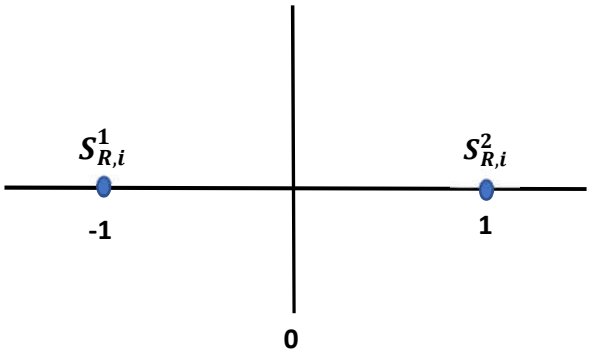

Figure 4.8: Normalized 2-PAM constellation.

$$s^1{}_{R,i}e^{2*}{}_{R,i}p\left(e^{2*}{}_{R,i}/s^1{}_{R,i}\right) = -1\left[2\,p\left(\hat{s}^1{}_{R,i} > 0\right)\right] = -2[\,p(e>1)] \\ = -2Q\left(\frac{1}{\sigma}\right) = -2Q\left(\sqrt{\frac{2}{2\,N_2}}\right) = -2Q\left(\sqrt{2\;\gamma_{sPAM}}\right). \quad (4.24)$$

Expression (4.24) is identical for the case when $k = 2$. This expectation is given by

$$E\left[s_{R,i}e^*{}_{R,i}\right] = \frac{1}{2}\left[-2Q\left(\sqrt{2\;\gamma_{sPAM}}\right) - 2Q\left(\sqrt{2\;\gamma_{sPAM}}\right)\right] = -2Q\left(\sqrt{2\;\gamma_{sPAM}}\right). \quad (4.25)$$

We can do similar calculations for $P-QAM = 16$, to get $\sqrt{P}-PAM = 4$ see Fig. 4.9 for this constellation where the expectation can be given by

$$E\left[s_{R,i}e^*{}_{R,i}\right] = \frac{-3}{5}\left[Q\left(\sqrt{\frac{2\;\gamma_{sPAM}}{5}}\right) + \frac{4}{3}Q\left(\sqrt{\frac{18\;\gamma_{sPAM}}{5}}\right) + Q\left(\sqrt{10\;\gamma_{sPAM}}\right)\right]. \quad (4.26)$$

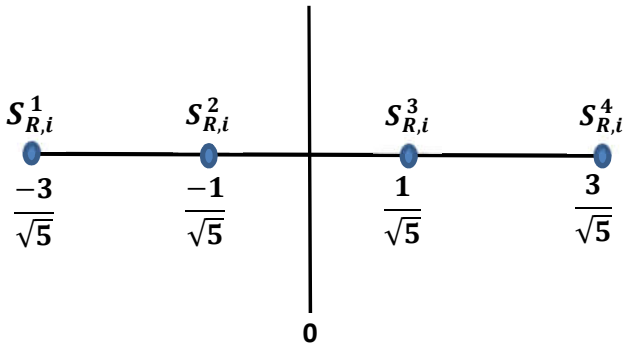

Figure 4.9: Normalized 4-PAM constellation.

Since $\gamma_{sPAM} = \frac{\gamma_{s\,QAM}}{2}$ to achieve the same probability of error, the expectation for QAM can be given for different sizes and is tabulated in Table 4.1

Table 4.1:Values $E[s_{R,i}e^{*}{}_{R,i}]$of for different constellations.

Constellation	$E[s_{R,i}e^{*}{}_{R,i}]$
64-QAM	$\frac{-1}{84}\left[14\,Q\left(\sqrt{\frac{\gamma_{s\,QAM}}{21}}\right)+30\,Q\left(\sqrt{\frac{25\;\gamma_{s\,QAM}}{21}}\right)+40\,Q\left(\sqrt{\frac{7\;\gamma_{s\,QAM}}{3}}\right)+30\,Q\left(\sqrt{\frac{27\;\gamma_{s\,QAM}}{7}}\right)+24\,Q\left(\sqrt{\frac{121\;\gamma_{s\,QAM}}{21}}\right)+24\,Q\left(\sqrt{\frac{3\;\gamma_{s\,QAM}}{7}}\right)+14\,Q\left(\sqrt{\frac{169\;\gamma_{s\,QAM}}{21}}\right)\right]$
16-QAM	$\frac{-3}{5}\left[Q\left(\sqrt{\frac{\gamma_{s\,QAM}}{5}}\right)+\frac{4}{3}Q\left(\sqrt{\frac{9\;\gamma_{s\,QAM}}{5}}\right)+\left(\sqrt{5\;\gamma_{s\,QAM}}\right)\right]$
4-QAM	$-2Q\left(\sqrt{\gamma_{s\,QAM}}\right)$

Finally, the feedback correlation metric will be calculated as follows:

$$r_{s,\hat{s}} = 1 + 2\,E[s_{R,i}e^{*}{}_{R,i}]. \tag{4.27}$$

4.2.1. Simulation Results

The simulation to test the new feedback correlation metric will be conducted here with the same previous parameters of SC-FDMA, PHN and channel environment given in chapter 3.

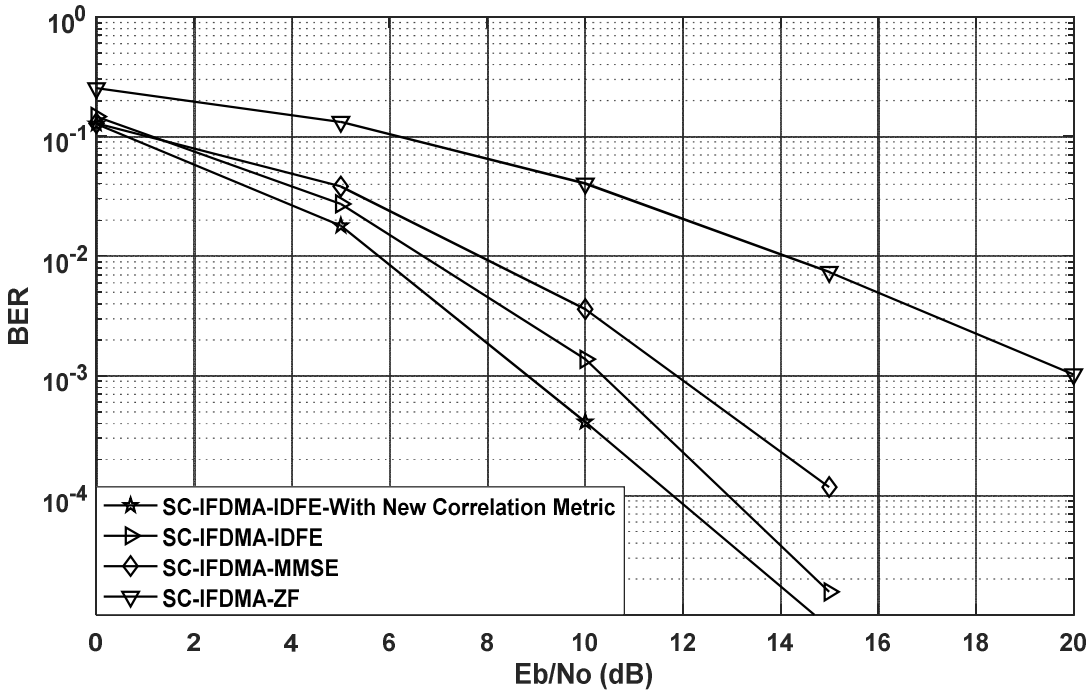

Figure 4.10:Comparison between various types of FD equalizers.

It is clear that, the Bit Error Rate (BER) performance of the Iterative-FD-E in Fig 4.10 in Vehicular A channel model will improve by using the new correlation metric, where we can achieve BER=10^{-4} at 11.5 dB Compared to 13 dB in the old Iterative-FD-E and 15 dB in the MMSE.

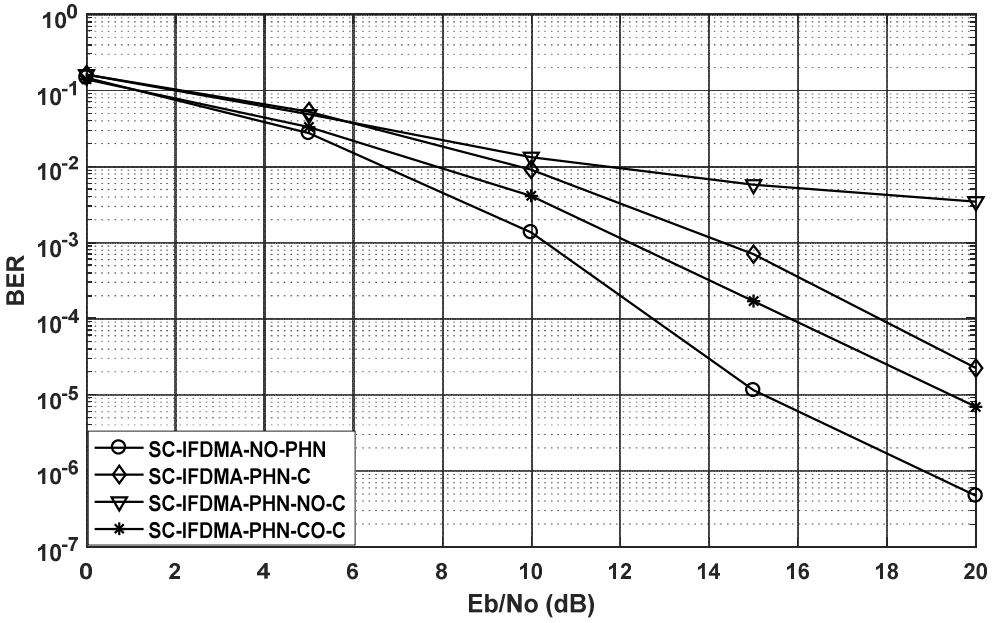

Figure 4.11: Iterative equalization and PHN compensation.

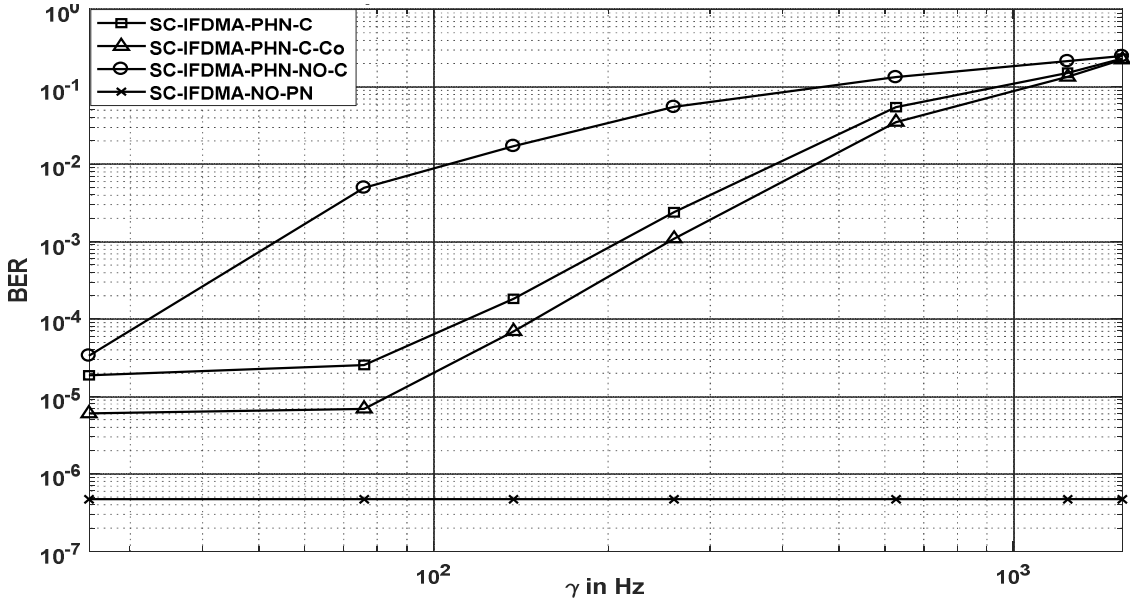

Figure 4.12: PHN compensation With correlation metric V.S PHN levels.

Also, from Fig. 4.11 and Fig. 4.12 we can note that the iterative-FD-E algorithm in PHN Compensation will improve also by utilizing new Correlation metric.

4.3. Conclusion

In this chapter, the iterative nature of the Iterative-FD-DFE in SC-FDMA to jointly eliminate ISI & compensate PHN simultaneously was improved by using a reliability procedure and new correlation metric. Also, the simulation results support our findings which are robustness and notable performance gain under critical conditions of the channels and transceiver PHN Levels.

CHAPTER 5

CONCLUSION AND FUTURE WORK

In this chapter, we summarize and discuss the main contributions of this thesis and suggest some possible future research directions.

5.1.Summary of Contributions

The main objective of this thesis was to study the combination of SC-FDMA FD-E and PHN mitigation iteratively. Then provide an improvement of the error propagation problem based on the reliability or correlation metric of the detected symbols in the feedback. The conclusion of the thesis can be summarized as follow:

1) In the situation when the multipath communication channel makes drastic ISI distortion, the LE cannot give adequate performance. Alternatively, a non-linear realization named a decision feedback equalizer (DFE) is needed, particularly when deep spectral nulls occurred in the frequency response of the channel. DFE provides Optimal SC-E algorithm due to its strength to remove post-cursor-ISI utilizing earlier recognized symbols. By the transition of the equalization process from the TD to the FD, the complexity of the computational complexity becomes low and much easier. By iterate the equalization process the error propagation will be restricted to only one data-block instead of propagating through all data-blocks. The slow variation and low-pass characteristics of PHN give us the possibility to estimate and compensate its effects iteratively. We employed the iterative nature of

the I-FD-DFE technique to combine the PHN compensation to the equalization process in a single algorithm.

2) The incorrect feedback decisions will become more serious especially in the deep fading environment that makes error propagate through the equalization process. Consequently, we propose a technique to improve the I-FD-DFE process based on the reliability of the detected symbols. The reliability criteria only rely on the relative measure of the distance between the received constellation point and its neighbors to find the confidence levels. After we get the reliability for each detected symbol, we pick and arrange the symbols with greatest reliability value in descending order and index them. Then the symbols with the highest reliability will be chosen in the decision feedback. Our simulation results prove our findings in vehicular A channel model.

3) Also, we can improve the I-FD-DFE by alleviating the effects of the incorrect feedback decisions by improving the calculation of the feedback correlation metric based on the assumption of Gaussian distribution of the output noise and considering the equivalency between QAM and PAM digital modulation techniques. Our simulation results prove our findings.

5.2. Future Work

As an extension of our work, we believe that if the PHN included in the derivation of the feed-forward and feed-back filters coefficients the system performance will be improved. Especially if we consider a way to estimate the variance of PHN effects such as CPE, ICI, and IUI.

References

[1] R. Nee and R. Prasad, OFDM for wireless multimedia communications. Artech House Publishers, 2000.

[2] W. Y. Zou and Y. Wu, "COFDM: an overview," IEEE Trans. Broadcast., vol. 41, no. 1, pp. 1–8, 1995.

[3] L. J. Cimini, "Analysis and simulation of a digital mobile channel using orthogonal frequency division multiplexing," IEEE Trans .Commun., vol. 33, no. 7, pp. 665–675, 1985.

[4] S. B. Weinstein and P. M. Ebert, "Data transmission by frequency-division multiplexing using the discrete fourier transform," IEEE Trans. Commun. Technol, vol. 19, no. 5, pp. 628–634, 1971.

[5] C. Y. Wong, R. S. Cheng, K. Ben Letaief, and R. D. Murch, "Multiuser OFDM with adaptive subcarrier bit and power allocation," IEEE J. Sel. Areas Commun., vol. 17, no. 10, pp. 1747–1758, 1999.

[6] I. Koffman and V. Roman, "Broadband wireless access solutions based on OFDM access in IEEE 802.16," IEEE Commun. Mag., vol. 40, no. 4, pp. 96–103, 2002.

[7] H. G., Myung, and D. J. Goodman, Single carrier FDMA: a new air interface for long term evolution. UK: John Wiley & Sons, Chichester, Ltd, 2008.

[8] Y. Yoshida, K. Hayashi, H. Sakai, and W. Bocquet, "Analysis and compensation of transmitter IQ imbalances in OFDMA and SC-FDMA systems," IEEE Trans. Signal

Process., vol. 57, no. 8, pp. 3119–3129, 2009.

[9] S. A. E.-D. and F. E. A. E.-S. Emad S. Hassan1, XuZhu2, Said E. El-Khamy, Moawad I. Dessouky, Department, J. Hernández-Serrano, and M. Soriano, "Securing cognitive radio networks," Int. J. Commun. Syst., vol. 23, no. 5, pp. 633–652, 2011.

[10] A. D. and V. Z. R. N. M. Bossert', "Impact of various parameters on the performance of free space optics communication system," Opt. - Int. J. Light Electron Opt., vol. 124, no. 22, pp. 5774–5776, Nov. 2013.

[11] F. Khan, LTE for 4G Mobile Broadband, America, vol. 129. 2009.

[12] G. K. Kaleh, "Channel equalization for block transmission systems," IEEE J. Sel. Areas Commun., vol. 13, no. 1 pt 2, pp. 110–121, 1995.

[13] M. V. Clark, "Adaptive frequency-domain equalization and diversity combining for broadband wireless communications," IEEE J. Sel. Areas Commun., vol. 348, no. 5, pp. 1385–1395, 1998.

[14] M. Tuchler and J. Hagenauer, "Linear time and frequency domain turbo equalization," IEEE VTS 53rd Veh. Technol. Conf. Spring 2001. Proc. (Cat. No.01CH37202), vol. 2, pp. 1449–1453, 2001.

[15] R. Dinis, D. Falconer, C. TongLam, and M. Sabbaghian, "Amultiple accessscheme for the uplinkof broadband wireless systems," IEEE Glob. Telecommun. Conf. 2004. GLOBECOM '04., vol. 6, no. 1, pp. 3808–3812, 2004.

[16] F. Pancaldi and G. M. Vitetta, "Block channel equalization in the frequency domain," IEEE

Trans. Commun., vol. 53, no. 3, pp. 463–471, 2005.

[17] N. Benvenuto and S. Tomasin, “Iterative design and detection of a DFE in the frequency domain,” IEEE Trans. Commun., vol. 53, no. 11, pp. 1867–1875, 2005.

[18] B. Ng, C. T. Lam, and D. Falconer, “Frequency domain equalization for single-carrier broadband wireless systems,” IEEE Commun. Mag., vol. 40, no. 2, pp. 58–66, 2002.

[19] A.Goldsmith., Wireless communications. Cambridge university press, 2005.

[20] G. Proakis, Digital Communications, Fourth ed. 2001.

[21] G. Proakis and M. Salehi, Communication Systems Engineering, 2nd Ed.,1994.

[22] V. Erceg et al., “A Model for the multipath delay profile of fixed wireless channels,” IEEE J. Sel. Areas Commun., vol. 17, no. 3, pp. 399–410, 1999.

[23] J. T. E. McDonnell and T. a. Wilkinson, “Comparison of computational complexity of adaptive equalization and OFDM for indoor wireless networks,” Proc. PIMRC ’96 - 7th Int. Symp. Pers. Indoor, Mob. Commun., vol. 3, pp. 1088–1091, 1996.

[24] M. V. Clark, “Adaptive frequency-domain equalization and diversity combining for broadband wireless communications,” IEEE J. Sel. Areas Commun., vol. 16, no. 8, pp. 1385–1395, 1998.

[25] E. G. Larsson and P. Stoica, “Space-time block coding for wireless communications,” Cambridge Univ. Press, Mar. 2008.

[26] E. Rubiola, “Phase Noise and Frequency Stability in Oscillators,” Cambridge Univ. Press, 2009.

[27] J. A. Crawford, Frequency Synthesizer Design Handbook. Artech House on Demand, 1994.

[28] D. M. Pozar, Microwave and RF design of wireless systems. Wiley Publishing, 2000.

[29] E. S. Ferre-Pikal et al., "Draft revision of IEEE STD 1139-1988 standard definitions of physical quantities for fundamental, frequency and time metrology-random instabilities," Proc. Int. Freq. Control Symp., pp. 338–357, 1997.

[30] S. Wu, P. Liu, and Y. Bar-Ness, "Phase noise estimation and mitigation for OFDM Systems," IEEE Trans. Wirel. Commun., vol. 5, no. 12, pp. 3616–3625, Dec. 2006.

[31] S. Wu and Y. Bar-Ness, "Computationally efficient phase noise cancellation technique in OFDM systems with phase noise," in Eighth IEEE International Symposium on Spread Spectrum Techniques and Applications - Programme and Book of Abstracts (IEEE Cat. No.04TH8738), 2004, pp. 788–792.

[32] D. Petrovic, W. Rave, and G. Fettweis, "Effects of phase noise on OFDM systems with and without PLL: characterization and compensation," IEEE Trans. Commun., vol. 55, no. 8, pp. 1607–1616, Aug. 2007.

[33] Y. Wan Kim and J. Du Yu, "Phase noise model of single loop frequency synthesizer," IEEE Trans. Broadcast., vol. 54, no. 1, pp. 112–119, Mar. 2008.

[34] A. Mehrotra, "Noise analysis of phase-locked loops," IEEE Trans. Circuits Syst. I Fundam. Theory Appl., vol. 49, no. 9, pp. 1309–1316, Sep. 2002.

[35] A. Demir, "Computing timing Jitter from phase noise spectra for oscillators and

phase-locked loops with white and 1/f noise," IEEE Trans. Circuits Syst. I Regul. Pap., vol. 53, no. 9, pp. 1869–1884, Sep. 2006.

[36] J. A. McNeill, "Jitter in ring oscillators," IEEE J. Solid-State Circuits, vol. 32, no. 6, pp. 870–879, Jun. 1997.

[37] A. Demir, A. Mehrotra, and J. Roychowdhury, "Phase noise in oscillators: a unifying theory and numerical methods for characterization," IEEE Trans. Circuits Syst. I Fundam. Theory Appl., vol. 47, no. 5, pp. 655–674, May 2000.

[38] A. Hajimiri and T. H. Lee, "A general theory of phase noise in electrical oscillators," IEEE J. Solid-State Circuits, vol. 33, no. 2, pp. 179–194, 1998.

[39] K. G. Paterson and V. Tarokh, "On the existence and construction of good codes with low peak-to-average power ratios," IEEE Trans. Inf. Theory, vol. 46, no. 6, pp. 1974–1987, 2000.

[40] N. Benvenuto, Algorithms for Communications Systems and their Applications. 2002.

[41] N. Benvenuto and S. Tomasin, "On the comparison between OFDM and single carrier modulation with a DFE using a frequency-domain feedforward filter," IEEE Trans. Commun., vol. 50, no. 6, pp. 947–955, 2002.

[42] C. Zhang, Z. Wang, Z. Yang, J. Wang, and J. Song, "Frequency Domain Decision Feedback Equalization for Uplink SC-FDMA," IEEE Trans. Broadcast., vol. 56, no. 2, pp. 253–257, Jun. 2010.

[43] 3GPP, "Physical Channels and Modulation," ETSI TS, vol. V10.0.0, no. 136.211,

2011.

[44] H. Witschnig, M. Kemptner, R. Weigel, and A. Springer, “Decision feedback equalization for a single carrier system with frequency domain equalization - an overall system approach,” 1st Int. Symp. onWireless Commun. Syst. 2004., pp. 26–30, 2004.

[45] G. Huang, A. Nix, and S. Armour, “Decision feedback equalization in SC-FDMA,” IEEE Int. Symp. Pers. Indoor Mob. Radio Commun. PIMRC, pp. 6–10, 2008.

[46] Y. C. Liang, S. Sun, and C. K. Ho, “Block-iterative generalized decision feedback equalizers for large MIMO systems: Algorithm design and asymptotic performance analysis,” IEEE Trans. Signal Process., vol. 54, no. 6 I, pp. 2035–2048, 2006.

[47] C. Zhang, Z. Wang, C. Pan, S. Chen, and L. Hanzo, “Low-complexity iterative frequency domain decision feedback equalization,” IEEE Trans. Veh. Technol., vol. 60, no. 3, pp. 1295–1301, 2011.

[48] Simon Haykin, Adaptive Filter Theory Prentice Hall, 3rd Editio. 1995.

[49] A. Garcia Armada and M. Calvo Ramon, “Rapid prototyping of a test modem for terrestrial broadcasting of digital television,” IEEE Trans. Consum. Electron., vol. 43, no. 4, pp. 1100–1109, 1997.

[50] A. G. A. Armada and M. Calvo, “Phase noise and sub-carrier spacing effects on the performance of an OFDM communication system,” IEEE Commun. Lett., vol. 2, no. 1, pp. 11–13, 1998.

[51] A. G. Armada, “Understanding the effects of phase noise in orthogonal frequency

division multiplexing OFDM," IEEE Trans. Broadcast., vol. 47, no. 2, pp. 153–159, 2001.

[52] D. Petrovic, W. Rave, and G. Fettweis, "Phase Noise Influence on Bit Error Rate, Cut-off Rate and Capacity of M-QAM OFDM Signaling," Int. OFDM-Workshop, Hambg., pp. 188–193, 2002.

[53] D. Petrovic, W. Rave, and G. Fettweis, "Performance degradation of coded-OFDM due to phase noise," 57th IEEE Semiannu. Veh. Technol. Conf. 2003. VTC 2003-Spring., vol. 2, no. 2, pp. 1168–1172.

[54] D. Petrovic, W. Rave, and G. Fettweis, "Phase noise suppression in OFDM including intercarrier interference," Int. OFDM Work., vol. 3, no. 1, pp. 219–224, 2003.

[55] A. Demir, A. Mehrotra, and J. Roychowdhury, "Phase noise in oscillators: a unifying theory and numerical methods for characterization," IEEE Transactions on Circuits and Systems, vol. 47, no. 5. pp. 655–674, 2000.

[56] D. Petrovic, W. Rave, and G. Fettweis, "Phase Noise Suppression in OFDM Using a Kalman Filter," Symp. Wirel. Pers. Multimed. Commun., 2003.

[57] D. Petrovic, W. Rave, and G. Fettweis, "Intercarrier interference due to phase noise in OFDM-estimation and suppression," Proc. IEEE VTC Fall, pp. 2191–2195, 2004.

[58] G. Fettweis, M. Löhning, D. Petrovic, M. Windisch, P. Zillmann, and W. Rave, "Dirty RF: A New Paradigm," Int. J. Wirel. Inf. Networks, vol. 14, no. 2, pp. 133–148, Jun. 2007.

[59] W. Rave, D. Petrovic, and G. Fettweis, “Iterative Correction of Phase Noise in Multicarrier Modulation,” Proc. 9th Int. OFDM Work., 2004.

[60] S. Wu and Y. Bar-Ness, “A phase noise suppression algorithm for OFDM-based WLANs,” IEEE Commun. Lett., vol. 6, no. 12, pp. 535–537, Dec. 2002.

[61] S. Wu and Y. Bar-ness, “OFDM Systems in the Presence of Phase Noise:consequences and solutions,” IEEE Transactions on Communications, vol. 52, no. 11, pp. 1988–1996, 2004.

[62] V. Syrjala and M. Valkama, “Receiver DSP for OFDM Systems Impaired by Transmitter and Receiver Phase Noise,” IEEE International Conference on Communications (ICC), 2011, no.11, pp. 1–6. July 2011.

[63] S. Bittner, W. Rave, and G. Fettweis, “Joint Iterative Transmitter and Receiver Phase Noise Correction using Soft Information,” IEEE International Conference on Communications, pp. 2847–2852, 2007.

[64] M. M. Rahman, M. D. Hossain, and A. B. M. S. Ali, “Performance Analysis of OFDM Systems with Phase Noise,” in 6th IEEE/ACIS International Conference on Computer and Information Science (ICIS 2007), no. Icis, pp. 358–362, 2007.

[65] P. Mathecken, T. Riihonen, S. Werner, and R. Wichman, “Performance Analysis of OFDM with Wiener Phase Noise and Frequency Selective Fading Channel,” IEEE Trans. Commun., vol. 59, no. 5, pp. 1321–1331, May 2011.

[66] V. Syrjala, “Modelling and practical iterative mitigation of phase noise in SC-FDMA,” in 2012 IEEE 23rd International Symposium on Personal, Indoor and

Mobile Radio Communications - (PIMRC), pp. 2395–2400, 2012.

[67] K. Nikitopoulos, S. Stefanatos, and A. K. Katsaggelos, “Decision-aided compensation of severe phase-impairment-induced inter-carrier interference in frequency-selective OFDM,” IEEE Trans. Wirel. Commun., vol. 8, no. 4, pp. 1614–1619, Apr. 2009.

[68] S. B. Ryu, J. Kim, and H. Ryu, “PNS Algorithm for the SC-FDMA Communication System with Phase Noise,” Wireless and Optical Communications Networks, 2009. WOCN'09. IFIP International Conference on. IEEE, 2009

[69] X. Zhang and H.-G. Ryu, “Joint estimation and suppression of phase noise and carrier frequency offset in multiple-input multiple-output single carrier frequency division multiple access with single-carrier space frequency block coding,” IET Commun., vol. 4, no. 16, p. 1998, 2010.

[70] A. Gomaa and N. Al-Dhahir, “SC-FDMA Performance in Presence of Oscillator Impairments: EVM and Subcarrier Mapping Impact,” in 2011 IEEE Global Telecommunications Conference - GLOBECOM 2011, 2011, pp. 1–5.

[71] G. Sridharan and T. J. Lim, “Performance analysis of SC-FDMA in the presence of receiver phase noise,” IEEE 22nd International Symposium on Personal, Indoor and Mobile Radio Communications, vol. 60, no. 12, pp. 1978–1982,2011.

[72] N. Alliance, “5G White Paper,” [Online]. Available: https://www.ngmn.org., 2015.

[73] Ş. Alphan, R. Yang, F. La Sita, and R. L. Olesen, “A Comparison of SC-FDE and UW DFT-s-OFDM for Millimeter Wave Communications,” IEEE Int. Conf.

Commun. (ICC), no. arXiv:1801.09177v1, pp. 1–7, 2018.

[74] Y. Sun, S. He, Y. Wang, H. Wang, Y. Huang, and L. Yang, “Phase noise mitigation for millimeter-wave SC-FDE MIMO systems,” Int. Conf. Wirel. Commun. Signal Process. WCSP 2015, 2015.

[75] S. Suyama, J. Onodera, H. Suzuki, and K. Fukawa, “Decision-directed phase noise compensation for millimeter-wave single carrier systems with iterative frequency-domain equalization,” Int. J. Microw. Wirel. Technol., vol. 2, no. 3–4, pp. 399–408, 2010.

[76] H. Sari, G. Karam, and I. Jeanclaude, “An analysis of orthogonal frequency-division multiplexing for mobile radio applications,” in Proceedings of IEEE Vehicular Technology Conference (VTC), pp. 1635–1639, 1994.

[77] ETSI, “Physical channels and modulation,” Ts 36.211 V12.6.0, vol. 10.0.0, pp. 0–137, 2015.

[78] J. G. Proakis, “Proakis J.G.-Digital Communications (2001).” p. 1015, 2001.

[79] N. Benvenuyo and G. Cherubini, Algorithms for Communications Systems & their Applications. 2002.

[80] Y. Zhu and K. Letaief, “Single Carrier Frequency Domain Equalization with Time Domain Noise Prediction for Wideband Wireless Communications,” IEEE Trans. Wirel. Commun., vol. 5, no. 12, pp. 3548–3557, Dec. 2006.

[81] T. Tang, Y. Li, and J. Wang, “Improved methods of decision feedback equalization for error propagation prevention,” Proc. 2014 9th IEEE Conf. Ind. Electron. Appl.

ICIEA 2014, pp. 1072–1076, 2014.

[82] J. E. Smee and N. C. Beaulieu, “Error-rate evaluation of linear equalization and decision feedback equalization with error propagation,” IEEE Trans. Commun., vol. 46, no. 5, pp. 656–665, May 1998.

[83] P. Mathecken, T. Riihonen, S. Werner, S. Member, and R. Wichman, “Constrained Phase Noise Estimation in OFDM Using Scattered Pilots Without Decision Feedback,” IEEE Trans. Signal Processing ,vol. 65, no. 9, pp. 2348–2362, 2017.

[84] M. Sabbaghian and D. Falconer, “Joint Turbo Frequency Domain Equalization and Carrier Synchronization,” IEEE Trans. Wirel. Commun., vol. 7, no. 1, pp. 204–212, Jan. 2008.

[85] C. Zhang, Z. Xiao, B. Gao, L. Su, and D. Jin, “Iterative Tx and Rx phase noise compensation for 60 GHz systems with SC-FDE transmission,” IEEE International Conference on Communications (ICC), pp. 5158–5162, 2013.

[86] A. M. Chan and G. W. Wornell, “A class of block-iterative equalizers for intersymbol interference channels: Fixed channel results,” IEEE Trans. Commun., vol. 49, no. 11, pp. 1966–1976, 2001.

[87] L. Tomba, “On the effect of Wiener phase noise in OFDM systems,” IEEE Trans. Commun., vol. 46, no. 5, pp. 580–583, May 1998.

[88] T. Schenk, RF Imperfections in High-rate Wireless Systems. Dordrecht: Springer Netherlands, 2008.

[89] T. Pollet, M. Van Bladel, and M. Moeneclaey, “BER sensitivity of OFDM systems

to carrier frequency offset and Wiener phase noise," IEEE Trans. Commun., vol. 43, no. 2–4 pt 1, pp. 191–193, 1995.

[90] P. Mathecken, T. Riihonen, S. S. Member, S. Werner, S. S. Member, and R. Wichman, "Performance analysis of OFDM with wiener phase noise and frequency selective fading channel," IEEE Trans. Commun., vol. 59, no. 5, pp. 1321–1331, 2011.

[91] V. Syrjälä and M. Valkama, "Receiver DSP for OFDM systems impaired by transmitter and receiver phase noise," IEEE Int. Conf. Commun., 2011.

[92] N. Iqbal and A. Zerguine, "AFD-DFE using Constraint-Based RLS and Phase Noise Compensation for Uplink SC-FDMA," IEEE Trans. Veh. Technol., vol. PP, no. 99, p. 1, 2016.

[93] A. Ali, O. Hammi, and T. Y. Al-Naffouri, "Compressed Sensing Based Joint-Compensation of Power Amplifier's Distortions in OFDMA Cognitive Radio Systems," IEEE J. Emerg. Sel. Top. Circuits Syst., vol. 3, no. 4, pp. 508–520, Dec. 2013.

[94] D. S. Owodunni, A. Ali, A. A. Quadeer, E. B. Al-Safadi, O. Hammi, and T. Y. Al-Naffouri, "Compressed sensing techniques for receiver based post-compensation of transmitter's nonlinear distortions in OFDM systems," Signal Processing, vol. 97, pp. 282–293, Apr. 2014.

[95] G. Karagiannidis and A. Lioumpas, "An Improved Approximation for the Gaussian Q-Function," IEEE Commun. Lett., vol. 11, no. 8, pp. 644–646, Aug.

2007.

Vitae

Name	: Mohamed Anbar Mohamed Omar
Nationality	: Egypt
Date of Birth	:5/20/1987
Email	: mohammed1987anbar@gmail.com
Address	:El maragha, Sohag, Egypt
Academic Background	: Bachelor of Electrical Engineering from Al Azhar University in May 2010